Phthalates Particle-Gas Partitioning of Inorganic Particles: Effect of Ventilation, Particle Size and Phthalates Adsorption Competition

Azad Bahrami

A Thesis

In the Department

of

Building, Civil and Environmental Engineering

Presented in Partial Fulfillment of the Requirements

For the Degree of

Doctor of Philosophy (Civil Engineering) at

Concordia University

Montreal, Quebec, Canada

October 2025

CONCORDIA UNIVERSITY

SCHOOL OF GRADUATE STUDIES

This is to certify that the thesis prepared

By: Azad Bahrami

Entitled: Phthalates Particle-Gas Partitioning of Inorganic Particles: Effect of Ventilation, Particle Size and Phthalates Adsorption Competition

and submitted in partial fulfillment of the requirements for the degree of

Doctor of Philosophy (Civil Engineering)

complies with the regulations of the University and meets the accepted standards with respect to originality and quality.

Signed by the final examining committee:

_____ Chair
Dr. Ahmed A. Kishk

_____ External Examiner
Dr. Ying Xu

_____ Arm's Length Examiner
Dr. Marius Paraschivoiu

_____ Examiner
Dr. Catherine Mulligan

_____ Examiner
Dr. Zhi Chen

_____ Thesis Supervisor
Dr. Fariborz Haghighat

_____ Thesis Co-Supervisor
Dr. Jiping Zhu

Approved by_____
Dr. Chunjiang An, Graduate Program Director

October 2025_____
Dr. Mourad Debbabi, Dean

Gina Cody School of Engineering & Computer Science

ABSTRACT

Phthalates Particle–Gas Partitioning of Inorganic Particles: Effect of Ventilation, Particle Size and Phthalates Adsorption Competition

Azad Bahrami. Ph.D.

Concordia University, 2025

Semi-volatile organic compounds (SVOCs) are widely used in building materials, personal consumer products, and furnishings. These compounds can have an interaction with ubiquitous particulate matters (PM) by particle-gas partitioning processes. This plays a critical role in human inhalation exposure; however, the influence of key indoor parameters such as ventilation rate (residence time), particle size, and competitive adsorption has been poorly documented.

The objective of this research is to systematically quantify the particle–gas partitioning of phthalates under controlled indoor conditions. Specifically, this study (i) evaluates the influence of ventilation rate (residence time), (ii) determines size-resolved partitioning behavior using monodisperse NaCl particles, and (iii) examines competitive adsorption between co-existing phthalates. Sodium chloride (NaCl) as a model inorganic particle and four phthalates covering a wide range of vapor pressure were selected. A mixing chamber was used to combine particles and phthalates under isolated conditions. Moreover, the performance of the existing particle-gas partitioning model (adsorption) was evaluated, highlighting its limitations when applied to indoor environments. The results showed that residence time (ventilation rate) can alter particle-gas partitioning (even for adsorption process), which was suggested to occur for only absorption

process (organic particles- or coated-particle). This can stem from higher interaction time between these two pollutants and might come from multilayer adsorption for longer interactions. For particles having size of 337 nm, 650 nm, and 1007 nm, results indicated that smaller particles tend to adsorb more SVOCs (in this case phthalates) on their surfaces. Furthermore, results showed that competitive adsorption in mixtures reduces individual compound uptake.

Not only do findings enhance the scientific understanding of SVOC partitioning behavior in indoor air, but also it offers new empirical insights that can refine predictive adsorption models. Besides, this study provides new methodological approaches for generating gaseous phthalates (including heavier species) which can be used for future works. Results have direct implication in exposure assessment, indoor air quality management, and the design of air remediation strategies. Lastly, this work supports the development of healthier indoor environments by providing data and modeling approaches better suited to real-world conditions.

ACKNOWLEDGMENT

I would like to express my highest gratitude to my supervisors, Professor Fariborz Haghighat and Dr. Jiping Zhu, for their outstanding guidance, wholehearted support, unwavering encouragement through my doctoral studies. It is by their sound counsel, constructive feedback, and scholarly expertise that I could develop my research skills, overcome challenges, and ultimately reach the level required to complete my PhD.

I am grateful to Dr. Jianjun Niu and Dr. Daryl Smith from Health Canada for their assistance and support.

I am deeply thankful to my thesis committee, Dr. Catherine Mulligan, Dr. Zhi Chen, Dr. Marius Paraschivoiu, and Dr. Ying Xu throughout the course of this research for their insightful feedback, guidance, and unwavering support, all which have been instrumental in shaping this research.

I am deeply grateful to my colleagues and friends (Mehrab Malekshahi, Mahsa Motamedi, Ali Asghar Sedighi, and Parham Haghighi) for their support and encouragement.

My heartfelt thanks go to my wife and my family. Their patience, encouragement, and constant support have sustained me throughout this journey, and this achievement would not have been possible without them.

Table of Contents

List of Tables

List of Figures

List of Symbols

Abbreviation	
AAS	Active air sampler
ADR	Acceptable data range
AER (1/h)	Air exchange rate
ATD	Automatic thermal desorber
CB	Carbon black
CPC	Condensation particle counter
EC	Elemental carbon
EDC	Endocrine disrupting chemical
EQ	Equilibrium domain
FLEC	Field and Laboratory Emission Cell
FRs	Flame retardants
GC/FID	Gas chromatography/flame ionization detection
GC/MS	Gas chromatography–mass spectrometry
GFF	Glass fiber filter
GPP	Gas-particle partitioning
HPLC	High-performance liquid chromatography
HVAS	High-volume air sampler
KL	Kanto Loam
LMW	Low-molecular-weight
L-M-Y	Li Ma Yang model
MFC	Mass flow controller
MOUDI	Micro-Orifice Uniform Deposit Impactor
MP	Maximum partition domain
MSD	Mass selective detector
NE	Non-equilibrium domain
OPE	Organophosphate ester
OPS	Optical Particle Sizer
PAE	Phthalate ester
PAH	Polycyclic aromatic hydrocarbon
PBDE	Polybrominated diphenyl ether
PCB	Polychlorinated biphenyl
PEM	Personal Environmental Monitor
PM	Particulate matter
pp-LFER	Poly-parameter linear free energy relationship
PTFE	Polytetrafluoroethylene
PUF	polyurethane foam
PVC	polyvinyl chloride
QFF	Quartz fiber filter
SMPS	Scanning mobility particle sizer
SOA	Secondary organic aerosol
SVOC	Semi-volatile organic compound

TD	Thermal desorption
TSP	Total suspended particle
VOC	Volatile organic compound
Chemicals	
BaP	Benzo(a)-pyrene
BBzP	Benzyl butyl phthalate
BDE-47	2,2',4,4'-Tetrabromodiphenyl ether
BDE-99	2,2',4,4',5-Pentabromodiphenyl ether
BDE-183	2,2',3,4,4',5',6-Heptabromodiphenyl ether
BDE-209	Decabromodiphenyl ether
DEHP	Di-2-ethylhexyl phthalate
DEP	Diethyl phthalate
DiBP	Diisobutyl Phthalate
DnBP	Di-n-butyl phthalate
FLT	Fluoranthene
Phe	Phenanthrene
PYR	Pyrene
Nomenclature	
A	Hydrogen-bond acidity
A_s (m^2)	Source surface areas
A_{ns} (m^2)	Non-source surface areas
A_p (m^2)	Surface area of a single particle
a_{EC} (m^2 surface/g adsorbent)	Adsorbent specific surface areas of elemental carbon/diesel soot
$a_{(NH_4)_2SO_4}$ (m^2 surface/g adsorbent)	Adsorbent specific surface areas of ammonium sulfate
a_{NH_4Cl} (m^2 surface/g adsorbent)	Adsorbent specific surface areas of ammonium chloride
B	Hydrogen-bond basicity
Bi_m	Biot number
C_g ($\mu g/m^3$)	Gas-phase SVOC concentration
C_J (Pa.cm)	Constant in Junge's equation
C_p ($\mu g/m^3$, mass of SVOCs/ volume of particles)	Particle-phase SVOC concentration
d_p (cm)	Particle diameter
f_{EC} ($g_{adsorbent}/g_{PM}$)	Fraction of elemental carbon, in particulate matter
$f_{(NH_4)_2SO_4}$ $g_{adsorbent}/g_{PM}$)	Fraction of ammonium sulfate in particulate matter
f_{NH_4Cl} ($g_{adsorbent}/g_{PM}$)	Fraction of ammonium chloride in particulate matter
f_{OM}	Fraction of organic matter on the particle

f_v	Volumetric fraction of permeable part of particles
$h_{m,p}$ (m/h)	Mass transfer coefficient of SVOC at particle surfaces
$h_{m,s}$ (m/h)	SVOC mass transfer coefficients for source surfaces
$h_{m,ns}$ (m/h)	SVOC mass transfer coefficients for non-source surfaces
K_{DMSO} (m^3_{air}/m^3_{DMSO})	Partitioning (absorption) coefficients for dimethyl sulfoxide-air
K_{EC} (mol $m^{-2}_{surface}$/mol m^{-3}_{air})	Partitioning (adsorption) coefficients for elemental carbon/diesel soot
$K_{(NH_4)_2SO_4}$ (mol $m^{-2}_{surface}$/mol m^{-3}_{air})	Partitioning (adsorption) coefficients for ammonium sulfate
K_{NH_4Cl} (mol $m^{-2}_{surface}$/mol m^{-3}_{air})	Partitioning (adsorption) coefficients for ammonium chloride
K_{OA}	Octanol-air partition coefficient
K_p ($m^3/\mu g$)	Gas-particle partitioning coefficient
K_{part} ($m^3/\mu g$)	Gas-particle partitioning quotient
K_{PU} (m^3_{air}/m^3_{PU})	Partitioning (absorption) coefficients for polyurethane-air
$K_{P\text{-}DE}$	Gas-particle partitioning coefficient of Dachs-Eisenreich
$K_{P\text{-}HB}$ ($m^3/\mu g$)	Gas-particle partitioning coefficient Harner and Bidleman model
$K_{P\text{-}L}$ ($m^3/\mu g$)	Gas-particle partitioning coefficient pp-LFER model
$K_{P\text{-}EC}$ ($m^3/\mu g$)	Adsorption term of gas-particle partitioning coefficient of Dachs-Eisenreich model
K_{SA} (L/Kg)	soot-air partition coefficient
L	Logarithmic hexadecane–air partition constant
N_p	Total number of suspended particles
N_{tsp} (#/cm^3)	Particle number concentration
$P_{dust,s}$ (μg/g)	Concentrations of SVOC in the settled dust on source surfaces
$P_{dust,ns}$ (μg/g)	concentrations of SVOC in the settled dust on non-source surfaces
P_L (Pa)	Vapor pressure of the sub-cooled liquid
Q (m^3/h)	Ventilation rate
R (J/mol.K)	Gas constant
R_p (1/h)	Particle resuspension rate
S	Dipolarity/polarizability of the substance

t (h)	Time
V	Molar volume
v_d (m/h)	Particle deposition velocity
y_0 ($\mu g/m^3$)	Gas concentration of SVOC adjacent to its source
y_{in} ($\mu g/m^3$)	Outdoor gas-phase SVOC
y_{ns} ($\mu g/m^3$)	Gas concentration of SVOC adjacent to non-source surfaces
Greek Symbols	
ΔH (J/mol)	Phase change enthalpy
θ (cm^2/cm^3)	Concentration of aerosol surface area
ρ_{DMSO} (g/m^3)	Dimethyl sulfoxide density
φ	Particulate-phase ratio

1 Introduction

1.1 Background

In modern life, humans spend most of their time (almost 90 %) in enclosed indoor environments such as residences, offices and schools (1). Poor indoor air quality can exert a significant influence on the occupants' health. Indoor air pollutants can significantly affect the quality of indoor air; they present in different phases: gases, vapors, and particulate matter (PM), of which the latter is suspended in a gaseous medium (2). These pollutants are generated either naturally (e.g., sea spray, mineral dust, smoke from wildfires) or anthropogenically (e.g. emission from building materials). Semi-volatile organic compounds (SVOCs) are among the most common indoor pollutants, owing to their widespread use as plasticizers, flame retardants, adhesives, and in many other applications in modern life (3). Many SVOCs can gradually be emitted from their primary sources as they are not chemically bound (4); moreover, they can infiltrate into buildings through ventilation and can distribute in the gas phase (see Figure 1.1). These compounds typically have higher molecular

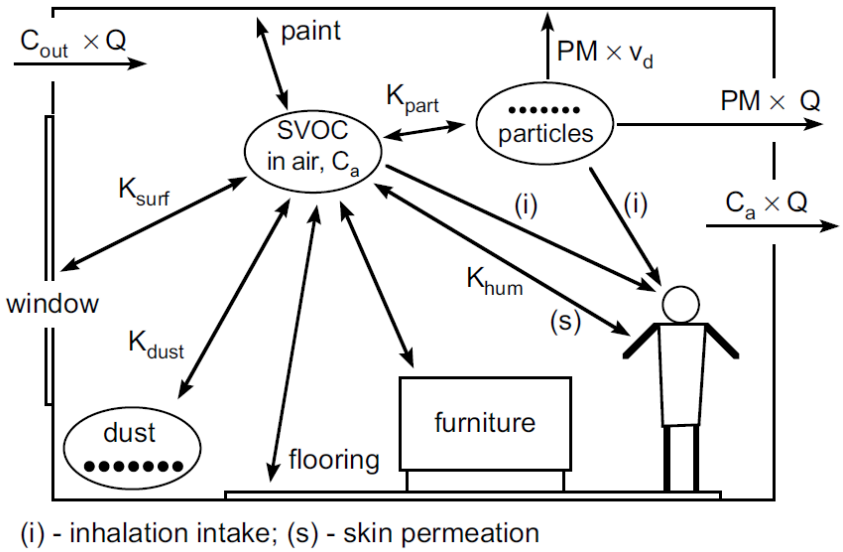

Figure 1.1. Schematic illustration of SVOC interaction with indoor compartments. The figure also depicts the SVOC exchanges with outdoor air through ventilation (5).

weights and higher boiling points than the volatile organic compounds (VOCs) (5). Unlike VOCs, SVOCs have lower vapor pressure, which increase their tendency to sorb onto (stick to) many indoor surfaces (e.g., airborne particles, settled dust, fixed surfaces, and human surfaces). This sorption makes them predominant indoor compounds for long periods even after removing their emission sources (6).

Among indoor surfaces, suspended particulate matter (PM) serves as a key solid phase for the sorption of SVOCs (7). As a result of interaction between particles and gaseous SVOCs (particle-gas partitioning), PM becomes another source of SVOC exposure by means of inhalation (8). Small particles such as PM2.5 can deeply penetrate into the respiratory system and in some cases to cardiovascular system causing pernicious impact on occupants' health (e.g., asthma, reproductive disorders, cancers, etc.) (9). Partitioned SVOCs on these particles can elevate such effects (10). A fraction of inhaled particle-associated SVOCs which reach the alveolar region can have the potential to enter the bloodstream and may reach key receptor sites. The particle size is a vital key to know where SVOCs can contact tissue in the respiratory system and to what extent they can affect metabolism (e.g. enzymatically promoted hydrolysis of phthalates). Therefore, improving our knowledge on this interaction is critical to better understanding SVOCs' behaviour in the indoor environment and to develop appropriate remediation strategies to reduce exposure to indoor SVOCs.

The interaction between SVOCs and particles is characterized by particle-gas partitioning coefficient (K_p), which describes how SVOCs distribute between the gas phase and particulate phases (11). This critical parameter can help us to assess indoor SVOCs behavior (their fate and transport), and human exposure risk, and it can help to improve indoor air quality modeling (12). In fact, applying measured K_p into mass balance models (following equations) can give

quantitative predictions that in which phase the SVOC will be (gas, particles, surfaces, dust), how long it suspends, and at what extent occupants will be exposed by inhalation, skin adsorption, or ingestion. Inside a well-mixed room with volume of V (m^3), the mass balance for total SVOC and particle-phase SVOC can be described as (13):

$$V\frac{dC_g}{dt} + V\frac{dC_p}{dt} = Q.(y_{in} + F_{in}) - Q.(C_g + C_p) + h_{m,s}.A_s.(y_0 - C_g) - h_{m,ns}.A_{ns}.(C_g - y_{ns}) - v_d.C_p.(A_s + A_{ns}) + RM_s.P_{dust,s}.A_s + RM_{ns}.P_{dust,ns}.A_{ns} \quad (1.1)$$

where t (h) is time, C_g (μg/m^3) and C_p (μg/m^3) are the gas-phase and particle-phase concentration of SVOC in room, respectively, and Q (m^3/h) is the ventilation rate. y_{in} (μg/m^3), F_{in} (μg/m^3) represent the gas-phase and particle-phase SVOC outdoor, respectively. $h_{m,s}$ (m/h) and $h_{m,ns}$ (m/h) are the mass transfer coefficients for source and non-source surfaces. y_0 (μg/m^3) is the gas concentration of SVOC adjacent to its source. A_s (m^2) and A_{ns} (m^2) are the source surface areas and non-source surfaces, respectively. y_{ns} (μg/m^3) is the gas-phase concentration adjacent to non-source surfaces, v_d (m/h) is the particle deposition velocity, R (1/h) is the particle resuspension rate, M_s (μg/m^2) and M_{ns} (μg/m^2) are the mass loading of settled dust on source and non-source surfaces, respectively. $P_{dust,s}$ (μg/g) and $P_{dust,ns}$ (μg/g) correspond to the concentrations of SVOC in the settled dust on source and non-source surfaces, respectively. By ignoring the diffusion of SVOC inside particles, the mass balance of particle-phase SVOC can be described as:

$$V\frac{dC_p}{dt} = Q.(F_{in} - F) + h_{m,p}.A_p.N\left(y - \frac{F}{K_p.TSP}\right) - v_d.F.(A_s + A_{ns}) + RM_s.P_{dust,s}.A_s + RM_{ns}.P_{dust,ns}.A_{ns} \quad (1.2)$$

where $H_{m,p}$ (m/h) corresponds to the mass transfer coefficient of SVOC at particle surfaces. A_p (m^2), N_p, and TSP ($\mu g/m^3$) represent the surface area of a single particle, the total number of suspended particles in the room, and the mass concentration of total suspended particles.

The particle-gas partitioning is a complex process governed by various factors including particle properties (particle size and particle composition) (14), SVOCs physiochemical properties (molecular weight, vapour pressure, polarity, and its compound group class) (15), and indoor environment conditions (air change rate, temperature, and humidity) (16). For example, particle composition has a direct effect on the partitioning process. SVOCs tend to partition to inorganic particles by adsorption, albeit into organic particles by absorption (17).

Particle-gas partitioning of SVOCs in atmospheric environment has been extensively studies, both experimentally (18,19) and through modelling work (20,21). Attempts have been made to correlate K_p with various parameters (depending on sorption mechanisms) such as vapour pressure of the compound (22) or octanol-air partitioning coefficient (a ratio that describes how a chemical distributes itself between octanol and air) of the compound (23) while some tried to describe the partitioning based on intermolecular interaction between gas and particles (e.g. van der Waals) (24). However, fewer studies have been conducted in indoor environment where its conditions is quite varied with outdoor settings (e.g. particle characteristics, ventilation patterns, and SVOCs sources).

For instance, limited research has pointed out how particle size, ventilation patterns, and multi-SVOCs competition for sorption can affect the partitioning coefficient. Furthermore, most models have developed based on assumptions on outdoor particles and condition (e.g. the sorption was described for both wet and dry conditions), which might not be applicable for indoor contexts. Therefore, more experimental data mimicking the real indoor environment is needed to evaluate

the dynamics of indoor particle-gas interactions accurately. This knowledge is vitally important in developing indoor air quality interventions and refining human exposure risk assessments, particularly in places where vulnerable groups such as children spend more time with direct contact with sources (kindergarten) or individual with pre-existing health conditions (hospital).

1.2 Problem statement

Indoor particle-gas partitioning can be affected by several factors. Ventilation rate, which can influence the interaction time between gaseous SVOCs and particles, has not been investigated. This impact is an important criterion to understand the behaviour of SVOCs in indoor air and have direct implications for air purification strategies. Another influential factor which has not been studied properly is particle size. Depending on particle sources, the mean particle size distribution will change. For example, cooking can produce both ultrafine (particles with a diameter smaller than 0.1 μm) and fine particles (with a diameter smaller than 2.5 μm) while candle burning is rich in ultrafine particles. By shifting from microscale to nanoscale, several key differences arise because of changes in physical and chemical properties such as surface area to volume, surface energy, and diffusivity etc. These changes can alter the affinity of particle to adsorb more SVOCs on its surface. However, except for very few field studies this parameter has not been considered. For example, the partitioning coefficient has been measured in a size-resolved study and showed that K_p values changed with particle size. However, such effect cannot be distinguished from other parameters like particle composition. This might be source of introducing potential bias into models using collected data from different locations where sources of particle might differ. Another issue in model is that the partitioning of particles and SVOCs have been described as a single-compound interaction. Nevertheless, in real indoor (or outdoor) environments, a complex

mixture of SVOCs is present and each compound depending on their affinity compete to settle on adsorption sites.

Despite development in both experimental and modeling studies, it is of the utmost importance to isolate parameters in experimental measurements to investigate effect of abovementioned parameters. In fact, no laboratory studies have been conducted to investigate the effect of particle size ranges, and ventilation scenarios on particle-gas partitioning process. Measuring K_p values in such conditions is crucial due to their direct use into indoor air quality and exposure models.

1.3 Research objectives

Based on abovementioned facts, the main objective of this work is to experimentally investigate the particle-gas partition behaviour of SVOCs on suspended inorganic particles under mimicked indoor conditions. Sodium chloride (NaCl) was selected as a model inorganic particle for its relatively easy to generate in different size ranges, its well-known density, which allows better control of particles' surface area at constant mass concentrations. To achieve this goal, the following research objectives were formulated:

1) Determine the influence of air change rate (residence time) on the indoor particle-gas partitioning behavior of SVOCs.

2) Determine the surface-area-related mechanisms using size-resolved inorganic NaCl particles.

3) Evaluate competitive adsorption effects among co-existing SVOCs on airborne particles.

1.4 Application

The proposed research will fill a critical knowledge gap by experimentally measuring the particle–gas partitioning coefficient of phthalates (a subgroup of SVOCs) across simulated indoor

conditions. The results will have wide practical impact on public health studies and indoor air quality management. Improving exposure assessment of indoor SVOCs leads to well-planned strategies to protect building occupants from hazardous indoor pollutants. Knowing the indoor behavior of SVOCs will help us to design and optimize the building ventilation and air cleaning systems to reduce the indoor SVOC concentrations.

1.5 Thesis outline

Chapter 1 (Introduction): This chapter presents an overview of the background of current research progress on particle-gas partition of SVOCs, existing problems that need to be studied, main objectives of the thesis research, and its application.

Chapter 2 (Literature review): This review provides a comprehensive review of SVOCs interaction with particulate matter in indoor environments. Its main focuses are on the particle-gas partitioning process, and how particle properties (e.g. particle size, composition and morphology) can regulate this interaction. Moreover, it summarizes both experimental and modeling studies (e.g. adsorption, absorption models and combination of both, equilibrium, and steady state models), which were used for describing the process in the state-of-the-art. The review also highlights the shortcomings of past studies, specifically the limitations of reporting particle physiochemical properties and sampling artifacts over the course of sampling, and it introduces the need for enhancing models and designing appropriate experiments in controlled conditions.

Chapter 3 (Methodology): Not only does this chapter describe detailed explanations of the experimental procedures and utilized setups illustrations, but also it presents a comprehensive explanation of the instrumentation calibration and analysis.

Chapter 4 (Influence of Air Exchange Rate on the Particle-Gas Partitioning of Phthalates onto Airborne Inorganic Particle): The focus of this chapter is on experimental investigation of how air exchange rate (AER)- a pivotal factor in ventilation- influences the particle-gas partitioning behavior of two phthalates onto inorganic NaCl particles. By fixing particle size and using a controlled mixing chamber, generated gaseous phthalates (introduced by single compound) are subjected to mix with generated particle at different residence time. This is followed by adsorption model validation for both compounds. In addition, an empirical model is developed to incorporate AER as factor in predicting K_p values, which provides better alignment with experimental data in comparison with traditional adsorption models where the effect of AER has been neglected.

Chapter 5 (Phthalates particle-gas partitioning of inorganic particles: Effect of particle size and phthalates adsorption competition): In this chapter, four phthalates are selected- covering a wide range of vapor pressure of the group to investigate the impact of particle size on the particle-gas partitioning. A novel approach is used to generate gaseous phthalates over the course of experiments- even for heavier compounds. Airborne particles are generated at different sizes while other parameters are isolated. The airflow is fixed for all compounds and configurations. K_p values are calculated by measuring particle concentration and both gas-phase and particle-phase phthalates and are compared with predicted values from traditional adsorption models. This study, furthermore, tries to improve models by calculating a constant introduced in model, which is a function of particle surface area concentration, over different particle sizes for four phthalates separately. This constant was used in previous atmospheric studies based on outdoor-based assumptions of particle surface area. Besides calculating K_p values for single-compound condition,

a binary mixture of two selected phthalates is introduced into the mixing chamber to examine the potential competition effects during adsorption process.

Chapter 6 (Conclusions and recommendations): This chapter offers a structured summary of the thesis findings, along with recommendations for future works.

1.6 Current thesis type

The current dissertation is a manuscript-based thesis in which chapters 2 to 5 are parts of the submitted or accepted journal papers in environmental engineering:

Chapter 2:

Azad Bahrami, Fariborz Haghighat, Jiping Zhu, "Indoor environment gas-particle partitioning models of SVOCs and impact of particle properties on the partitioning: A review." Building and Environment (2024): 111791

Chapters 3 & 4:

Azad Bahrami, Fariborz Haghighat, Jiping Zhu, Jianjun Niu, "Influence of Residence Time on the Particle-Gas Partitioning of Phthalates onto Airborne Inorganic Particle." Atmospheric Environment (2025): 121651

Chapters 3 & 5:

Azad Bahrami, Fariborz Haghighat, Jiping Zhu, Jianjun Niu, "Phthalates particle-gas partitioning of inorganic particles: Effect of particle size and phthalates adsorption competition." Building and Environment (2025): 113619

2 Literature Review

2.1 Gas-particle partition models

Gas-particle partitioning (GPP) of SVOCs has been mostly expressed in equilibrium state, meaning that the exchange process of SVOCs molecules from sources with the sorption sink (particulate matter or dust in this case) are balanced. In indoor spaces where mass and energy are perpetually exchanging, equilibrium partitioning may not be expected to achieve, particularly for compounds with higher octanol-air partition coefficient (K_{OA}) values; in fact, for these compounds slow sorption may take place where the sorption subjected to take more than 10 hours, whereas the time scale of air-exchange is less than few hours (25). Another approach to model the partitioning is through expressing the exchange process as a steady state (26), where sum of all source terms balances the sum of all sink terms. Besides, empirical models have been developed to explain the gas-particle interaction through a molecular mechanism based on the neutral electronic ground state (27). In this article, we selected 12 compounds from 3 SVOCs groups, including phthalic acid esters (PAEs), polybrominated diphenyl ethers (PBDEs), and polycyclic aromatic hydrocarbons (PAHs). Their relevant physicochemical properties are presented in Table 2.1.

Table 2.1. Physiochemical properties of selected compounds (25)

Chemical	CAS NO.	Molecular weight (g/mol)	Vapor pressure (Pa)	Log K_{OA}
DnBP	84−74−2	278.4	4.73×10^{-3}	8.54
DiBP	84−69−5	278.4	4.73×10^{-3}	8.54
BBzP	85−68−7	312.4	2.49×10^{-3}	8.78
DEHP	117−81−7	390.6	2.52×10^{-5}	10.53
BDE-47	5436-43-1	485.79	3.09×10^{-4}	10.53
BDE-99	60348-60-9	564.68	3.98×10^{-5}	11.31

BDE-183	207122-16-5	722.48	8.12×10^{-7}	12.78
BDE-209	163-19-5	959.16	3.98×10^{-10}	15.09
Phe	85-01-8	178.23	8.74×10^{-2}	7.22
FLT	206-44-0	202.26	8.10×10^{-3}	8.60
PYR	129-00-0	202.26	1.06×10^{-2}	8.19
BaP	50-32-8	252.32	2.30×10^{-5}	10.5

2.1.1 Gas/Particle partition coefficient

There are two ways to describe the partition coefficient. The first way is to use gas-particle partitioning coefficient (K_p) as following: (28,29)

$$K_p = \frac{C_p/TSP}{C_g} \tag{2.1}$$

where C_p is the particle-phase concentration of the SVOC TSP is the total suspended particles (mass/volume-μg/m^3), and C_g is the gas-phase concentration of the target SVOC (mass/volume-μg/m^3).

The second way is to use particulate-phase ratio, φ, which can be experimentally derived from the following equation:

$$\varphi = \frac{C_p}{C_p + C_g} \tag{2.2}$$

2.1.2 Experimental approaches to measure partition coefficient

Many studies have calculated K_p values using measurement data. A summary of earlier experimental work is presented in Table 2.2. These studies attempted to measure the gas- and particle-phase concentration of SVOCs and provided general information on K_p values For example, He et al. mentioned that the seasonality of K_p for specific compounds exhibits varying values (30). Wang et al. using a nano Micro-Orifice Uniform Deposit Impactor (nano-MOUDI),

revealed size distributions of PAHs and PAEs, and varied K_p suggesting different mechanisms influencing the partitioning of SVOCs in different particle size modes (14). The variation in reported K_p values for a specific compound in the table is attributed to differences in sampling conditions and variations in particle properties during the sampling process.

Moreover, factors like artifacts and breakthrough of gas or particles can overestimate or underestimate the exact value of K_p (31). In fact, sampling errors from the interaction of SVOCs and sorbent stem from two mechanisms: 1) The process of particulate-phase SVOCs becoming volatile, undergoing a shift into the gas phase from the sample (negative artifact leading to underestimate the particle-phase concentration and overestimation of gas-phase), and 2) Adsorption of gas-phase SVOCs on the filter (positive artifact resulting in underestimation of gas-phase concentration) (32,33). Besides, most of these works measured only concentrations and they did not characterize the factors that may influence the GPP process, such as particle size, particle composition, particle morphology etc. Therefore, when it comes to modeling the partitioning and predicting the particle-phase concentration, without these characterizations, one cannot compare data because they cannot tell which process was dominant (adsorption, absorption, or both).

Benning et al. for the first time conducted an experimental approach to measure K_p of DEHP toward ammonium sulfate (an inorganic particle). Generated particles were introduced to a chamber in which a DEHP-containing vinyl flooring were installed. Gaseous and total DEHP were measured separately by two Tenax sorbent tubes, one loaded with a polytetrafluoroethylene (PTFE) membrane to collect gaseous DEHP only, and another one without the filter to sample the total DEHP. They showed that an increase in particle concentration led to an increase in DEHP concentration emitted from a vinyl flooring (34). Later, Wu et al. developed a tube chamber with almost the same collection method as used by Benning et al. to experimentally study and compare

DEHP K_p value of organic and inorganic particles. The authors argued that the partitioning is expected to be dominated by adsorption for the inorganic particles and absorption for the organic particles (35). The results showed that K_p for organic particles was an order of magnitude higher than that for the inorganic particles of ammonium sulfate (Table 2.2).

Table 2.2. Summary of experimental works on measuring gas-particle partition coefficient (K_p) of three SVOCs groups: PAEs, PBDEs and PAHs.

Compound		Particle characteristics		SVOC analysis methods		K_p ($m^3/\mu g$)	Conditions	Limitations	Ref.
		Source	Size (μm)	Collection	Measurement				
Phthalates	DnBP	Residential indoor air environment	2.5>	PEM 2.5 PUF	GC/MS	1.0×10^{-2} 4.0×10^{-3}	The coefficient corresponds to summer and winter value. Indoor temperature during summer and winter was reported at 28.5 and 22.7 °C, respectively.	The particle distribution size was not involved. Particle composition was not considered, although it was suggested as a reason for coefficient difference in two seasons.	(36)

	-Indoor cooking -Indoor smoking -Outdoor haze	>18 10-18 5.6-10 3.2-5.6 1.8-3.2 1-1.8 0.56-1 0.32-0.56 0.18-0.32 0.1-0.18 0.056-0.1	MOUDI PUF	GC/MS	$3.3 \times 10^{-4} – 7.5 \times 10^{-3}$ $3.0 \times 10^{-4} – 5.2 \times 10^{-3}$ $1.9 \times 10^{-4} – 3.1 \times 10^{-3}$ $1.6 \times 10^{-4} – 2.3 \times 10^{-3}$ $1.8 \times 10^{-4} – 2.1 \times 10^{-3}$ $1.1 \times 10^{-4} – 1.4 \times 10^{-3}$ $1.0 \times 10^{-4} – 1.5 \times 10^{-3}$ $1.8 \times 10^{-4} – 2.1 \times 10^{-3}$ $3.8 \times 10^{-4} – 6.6 \times 10^{-3}$ $5.3 \times 10^{-4} – 7.4 \times 10^{-3}$ $7.5 \times 10^{-4} – 1.3 \times 10^{-2}$	Particle sample underwent three separate ultrasonic extractions, and each gaseous sample was subjected to Soxhlet extraction.	Although three particle sources were collected, the effect of composition on the partitioning was not studied. The effect of sampling bias was not considered.	(14)
DiBP	Residential indoor air environment	2.5>	PEM 2.5 PUF	GC/MS	5.3×10^{-2} 1.1×10^{-2}	The coefficient corresponds to summer and winter value. Indoor temperature during summer and winter was reported at 28.5 and 22.7 °C, respectively.	The particle distribution size was not involved. Particle composition was not considered, although it was suggested as a reason for coefficient difference in two seasons.	(36)

-Indoor	>18	MOUD	GC/MS	$3.4 \times 10^{-4} – 7.2 \times 10^{-3}$	Particle sample	Although three particle	(14)
cooking	10-18	I		$3.0 \times 10^{-4} – 5.2 \times 10^{-3}$	underwent three	sources were collected, the	
-Indoor	5.6-10	PUF		$1.9 \times 10^{-4} – 3.1 \times 10^{-3}$	separate ultrasonic	effect of composition on	
smoking	3.2-5.6			$1.8 \times 10^{-4} – 2.1 \times 10^{-3}$	extractions, and each	the partitioning was not	
-Outdoor	1.8-3.2			$1.9 \times 10^{-4} – 1.9 \times 10^{-3}$	gaseous sample was	studied. The effect of	
haze	1-1.8			$1.1 \times 10^{-4} – 1.3 \times 10^{-3}$	subjected to Soxhlet	sampling bias was not	
	0.56-1			$8.5 \times 10^{-5} – 1.1 \times 10^{-3}$	extraction.	considered.	
	0.32-0.56			$2.1 \times 10^{-4} – 1.8 \times 10^{-3}$			
	0.18-0.32			$3.0 \times 10^{-4} – 5.2 \times 10^{-3}$			
	0.1-0.18			$5.4 \times 10^{-4} – 7.2 \times 10^{-3}$			
	0.056-0.1			$7.9 \times 10^{-4} – 1.2 \times 10^{-2}$			

BBzP	-Indoor cooking -Indoor smoking -Outdoor haze	>18 10-18 5.6-10 3.2-5.6 1.8-3.2 1-1.8 0.56-1 0.32-0.56 0.18-0.32 0.1-0.18 0.056-0.1	MOUDI PUF	GC/MS	$3.0 \times 10^{-3} – 1.3 \times 10^{-1}$ $4.0 \times 10^{-3} – 1.5 \times 10^{-1}$ $1.9 \times 10^{-3} – 8.3 \times 10^{-2}$ $2.2 \times 10^{-3} – 7.0 \times 10^{-2}$ $2.6 \times 10^{-3} – 9.5 \times 10^{-2}$ $1.7 \times 10^{-3} – 5.7 \times 10^{-2}$ $1.2 \times 10^{-3} – 8.1 \times 10^{-2}$ $1.7 \times 10^{-3} – 1.4 \times 10^{-1}$ $5.7 \times 10^{-3} – 1.7 \times 10^{-1}$ $7.9 \times 10^{-3} – 1.9 \times 10^{-1}$ $1.4 \times 10^{-2} – 2.6 \times 10^{-1}$	Particle sample underwent three separate ultrasonic extractions, and each gaseous sample was subjected to Soxhlet extraction.	Although three particle sources were collected, the effect of composition on the partitioning was not studied. The effect of sampling bias was not considered.	(14)
DEHP	$(NH_4)_2SO_4$	0.045	PTFE Tenax tube	ATD and GC-FID	3.2×10^{-2}	Temperature was 22 °C. Ammonium sulfate particles were generated by using a constant output atomizer at 35 psi. A vinyl flooring was installed in a chamber for generating DEHP.	Limited to only one type of particle, one range of particle size and one surface area of the airborne particles.	(34)

Oleic acid Squalene Ammonium sulfate	0.04-0.13 0.11-0.17 0.07-0.08	PTFE Tenax tube	Particles: SMPS with CPC. DEHP: ATD, and GC-FID	$1.0 \times 10^{-1} – 3.6 \times 10^{-1}$ $1.0 \times 10^{-2} – 2.1 \times 10^{-1}$ $7.0 \times 10^{-3} – 1.8 \times 10^{-2}$	Organic particles were generated using a vaporization−condensation approach. Inorganic particles were generated using an atomizer. A slim layer of pure DEHP liquid, acting as the emission source, was meticulously coated onto the inner wall of a stainless-steel tube.	Given that achieving equilibrium partitioning may not be feasible in reality, non-equilibrium condition studies is needed. The particle morphology was assumed to be spherical and monodisperse. The particle size range for inorganic particle was lower than organic ones. A comparable range size is needed.	(35)

Residential indoor air environment	2.5> 2.5 PUF		GC/MS	2.1×10^{-2} 2.5×10^{-2}	The coefficient corresponds to summer and winter value. Indoor temperature during summer and winter was reported at 28.5 and 22.7, respectively.	The particle distribution size was not involved. Particle composition was not considered, although it was suggested as a reason for coefficient difference in two seasons.	(36)
-Indoor cooking -Indoor smoking -Outdoor haze	>18 10-18 5.6-10 3.2-5.6 1.8-3.2 1-1.8 0.56-1 0.32-0.56 0.18-0.32 0.1-0.18 0.056-0.1	MOUDI PUF	GC/MS	$3.0 \times 10^{-4} – 2.0 \times 10^{-2}$ $3.4 \times 10^{-4} – 1.8 \times 10^{-2}$ $2.3 \times 10^{-4} – 1.0 \times 10^{-2}$ $2.5 \times 10^{-4} – 1.0 \times 10^{-2}$ $3.0 \times 10^{-4} – 1.3 \times 10^{-2}$ $2.6 \times 10^{-4} – 9.3 \times 10^{-3}$ $2.2 \times 10^{-4} – 1.0 \times 10^{-2}$ $3.3 \times 10^{-4} – 1.2 \times 10^{-2}$ $2.8 \times 10^{-4} – 2.1 \times 10^{-2}$ $4.1 \times 10^{-4} – 2.3 \times 10^{-2}$ $3.7 \times 10^{-4} – 2.6 \times 10^{-2}$	Particle sample underwent three separate ultrasonic extractions, and each gaseous sample was subjected to Soxhlet extraction.	Although three particle sources were collected, the effect of composition on the partitioning was not studied. Effect of sampling bias was not considered.	(14)

Polybrominated Diphenyl Esthers	BDE-47	Rural outdoor air	NA	GFF PUF	GC/MS	$8.9 \times 10^{-4} – 2.7 \times 10^{-3}$	GFFs and PUF plugs were preprocessed, stored, and transported under specific conditions, and samples were collected, and analyzed for PMs and PBDEs, involving various extraction and purification.	Particle's properties were not documented. Effect of temperature on K_p and breakthrough was not studied.	(37)

Indoor air environment	PM_{10} PM_1	GFF PUF	GC/MS	3.5×10^{-2} 1.5×10^{-1}	Gas phase was sampled by active and passive sampling. Particulate phase samples were collected with the active gas phase sampling. An impactor was used for PM_{10} and PM_1 collection.	Particle composition was not documented, and effect of artifact was not considered.	(38)
Rural outdoor air	PM_{10}	GFF PUF	GC/MS	1.1×10^{-2} –3.3×10^{-2} 3.4×10^{-2} – 6.9×10^{-2} 7.5×10^{-3} – 4.5×10^{-2} 1.7×10^{-2} – 6.7×10^{-2}	Calculated based on atmospheric concentrations. Values show the GPP for each season, respectively.	Effect of temperature on sampling bias was not studied. Particle's properties were not documented.	(30)

	BDE-99	Rural outdoor air	NA	GFF PUF	GC/MS	$3.0 \times 10^{-3} – 8.9 \times 10^{-3}$	GFFs and PUF plugs were preprocessed, stored, and transported under specific conditions, and samples were collected, and analyzed for PMs and PBDEs, involving various extraction and purification.	Particle's properties were not documented. Effect of temperature on K_p and breakthrough was not studied.	(37)

Indoor air environment	PM_{10} PM_1	GFF PUF	GC/MS	3.3×10^{-2} 1.3×10^{-1}	Gas phase was sampled by active and passive sampling. Particulate phase samples were collected with the active gas phase sampling. An impactor was used for PM_{10} and PM_1 collection.	Particle composition was not documented, and effect of artifact was not considered.	(38)

	BDE-183	Rural outdoor air	NA	GFF PUF	GC/MS	$3.4 \times 10^{-2} – 1.3 \times 10^{-1}$	GFFs and PUF plugs were preprocessed, stored, and transported under specific conditions, and samples were collected, and analyzed for PMs and PBDEs, involving various extraction and purification.	Particle's properties were not documented. Effect of temperature on K_p and breakthrough was not studied.	(37)

Indoor air environment	PM_{10} PM_1	GFF PUF	GC/MS	3.0×10^{-2} 1.9×10^{-1}	Gas phase was sampled by active and passive sampling. Particulate phase samples were collected with the active gas phase sampling. An impactor was used for PM_{10} and PM_1 collection.	Particle composition was not documented, and effect of artifact was not considered.	(38)

BDE-209	Rural outdoor air	NA	GFF PUF	GC/MS	$7.1 \times 10^{-2} – 1.0 \times 10^{-1}$	GFFs and PUF plugs were preprocessed, stored, and transported under specific conditions, and samples were collected, and analyzed for PMs and PBDEs, involving various extraction and purification.	Particle's properties were not documented. Effect of temperature on K_p and breakthrough was not studied.	(37)

Indoor air environment	PM_{10} PM_1	GFF PUF	GC/MS	3.8×10^{-2} 1.7×10^{-1}	Gas phase was sampled by active and passive sampling. Particulate phase samples were collected with the active gas phase sampling. An impactor was used for PM_{10} and PM_1 collection.	Particle composition was not documented, and effect of artifact was not considered.	(38)
Rural outdoor air	PM_{10}	GFF PUF	GC/MS	$1.9 \times 10^{-2} – 9.7 \times 10^{-2}$ $1.7 \times 10^{-2} – 2.6 \times 10^{-2}$ $5.3 \times 10^{-3} – 4.6 \times 10^{-1}$ $1.8 \times 10^{-2} – 3.3 \times 10^{-1}$	Calculated based on atmospheric concentrations. Values show the GPP for each season, respectively.	Effect of temperature on sampling bias was not studied. Particle's properties were not documented.	(30)

Polycyclic Aromatic Hydrocarbons	Phe	Urban outdoor aerosol	PM_{10}	PTFE-coated GFF PUF	GC/MS	1.5×10^{-3} (summer) 1.9×10^{-3} (winter)	Filters were weighted before and after sampling to measure particle mass.	Sampling bias was not mentioned. Effect of temperature on artifacts was not included.	(39)
		Mining outdoor air	NA	QFF PUF	HPLC	$4.6 \times 10^{-5} – 3.7 \times 10^{-3}$	QFFs were ultrasonically extracted with n-hexane-DCM, while PUF plugs underwent extraction with Soxhlet, and both extracts were cleaned using liquid-solid chromatography.	Particle" properties were not studied. Sampling bias and effect of temperature on the bias were not included.	(40)

Urban outdoor air	PM_{10}	GFF PUF	GC/MSD	$8.1 \times 10^{-6} – 2.2 \times 10^{-4}$ (summer) 9.7×10^{-5} - 1.2×10^{-3} (winter)	PUF plugs and GFFs were Soxhlet extracted for 4 h and 10 h, respectively, and the concentrated extracts were analyzed.	Particle" properties were not studied. Sampling bias and effect of temperature on the bias were not included.	(41)
Urban outdoor air	4-6 0.9-1.2 0.4-0.45 0.13-0.17 ~0.05	Nano-MOUDI Al Foil	TD-GC/MS	1.1×10^{-4} 1.9×10^{-4} 6.7×10^{-5} 5.4×10^{-5} 2.9×10^{-5}	Sampling was conducted in different temperature. PAHs collected on Al foils were analyzed using in-injection port thermal desorption coupled with GC/MS.	Effect of temperature on GPP is not considered. Sampling bias was not documented.	(42)

	-Indoor cooking -Indoor smoking -Outdoor haze	>18 10-18 5.6-10 3.2-5.6 1.8-3.2 1-1.8 0.56-1 0.32-0.56 0.18-0.32 0.1-0.18 0.056-0.1	MOUDI PUF	GC/MS	$4.6 \times 10^{-6} – 8.5 \times 10^{-5}$ $4.2 \times 10^{-6} – 5.8 \times 10^{-5}$ $3.3 \times 10^{-6} – 4.6 \times 10^{-5}$ $4.1 \times 10^{-6} – 3.8 \times 10^{-5}$ $6.1 \times 10^{-6} – 4.1 \times 10^{-5}$ $6.9 \times 10^{-6} – 3.6 \times 10^{-5}$ $7.5 \times 10^{-6} – 5.2 \times 10^{-5}$ $9.7 \times 10^{-6} – 6.4 \times 10^{-5}$ $1.2 \times 10^{-5} – 1.2 \times 10^{-4}$ $1.6 \times 10^{-5} – 1.5 \times 10^{-4}$ $1.5 \times 10^{-4} – 2.5 \times 10^{-4}$	Particle sample underwent three separate ultrasonic extractions, and each gaseous sample was subjected to Soxhlet extraction.	Although three particle sources were collected, the effect of composition on the partitioning was not studied. Effect of sampling bias was not considered.	(14)
FLT	Urban outdoor aerosol	PM_{10}	PTFE-coated GFF PUF	GC/MS	6.3×10^{-3} (summer) 1.2×10^{-2} (winter)	Filters were weighed before and after sampling to measure particle mass.	Sampling bias was not mentioned. Effect of temperature on artifacts was not included.	(39)

Mining outdoor air	NA	QFF PUF	HPLC	$1.3 \times 10^{-3} – 2.9 \times 10^{-2}$	QFFs were ultrasonically extracted with n-hexane-DCM, while PUF plugs underwent extraction with Soxhlet, and both extracts were cleaned using liquid-solid chromatography.	Particle" properties were not studied. Sampling bias and effect of temperature on the bias were not included.	(40)
Urban outdoor air	PM_{10}	GFF PUF	GC/MSD	$2.8 \times 10^{-4} – 3.7 \times 10^{-3}$ (summer) $1.6 \times 10^{-3} – 2.7 \times 10^{-2}$ (winter)	PUF plugs and GFFs were Soxhlet extracted for 4 h and 10 h, respectively, and the concentrated extracts were analyzed.	Particle" properties were not studied. Sampling bias and effect of temperature on the bias were not included.	(41)

Urban	4-6	Nano-	TD-	1.2×10^{-3}	Sampling was	Effect of temperature on	(42)
outdoor	0.9-1.2	MOUD	GC/MS	2.0×10^{-3}	conducted in different	GPP is not considered.	
air	0.4-0.45	I		7.1×10^{-4}	temperature. PAHs	Sampling bias was not	
	0.13-0.17	Al Foil		5.7×10^{-4}	collected on Al foils	documented.	
	~0.05			3.1×10^{-4}	were analyzed using		
					in-injection port		
					thermal desorption		
					coupled with GC/MS.		
-Indoor	>18	MOUD	GC/MS	$3.4 \times 10^{-5} – 4.5 \times 10^{-4}$	Particle sample	Although three particle	(14)
cooking	10-18	I		$3.1 \times 10^{-5} – 3.2 \times 10^{-4}$	underwent three	sources were collected, the	
-Indoor	5.6-10	PUF		$4.2 \times 10^{-5} – 2.3 \times 10^{-4}$	separate ultrasonic	effect of composition on	
smoking	3.2-5.6			$6.6 \times 10^{-5} – 3.8 \times 10^{-4}$	extractions, and each	the partitioning was not	
-Outdoor	1.8-3.2			$1.3 \times 10^{-4} – 7.4 \times 10^{-4}$	gaseous sample was	studied. Effect of sampling	
haze	1-1.8			$1.9 \times 10^{-4} – 7.9 \times 10^{-4}$	subjected to Soxhlet	bias was not considered.	
	0.56-1			$2.3 \times 10^{-4} – 1.1 \times 10^{-3}$	extraction.		
	0.32-0.56			$2.8 \times 10^{-4} – 1.4 \times 10^{-3}$			
	0.18-0.32			$2.2 \times 10^{-4} – 1.7 \times 10^{-3}$			
	0.1-0.18			$2.5 \times 10^{-4} – 2.5 \times 10^{-3}$			
	0.056-0.1			$1.1 \times 10^{-4} – 2.1 \times 10^{-3}$			

PYR	Urban outdoor aerosol	PM_{10}	PTFE-coated GFF PUF	GC/MS	1.0×10^{-2} (summer) 1.5×10^{-2} (winter)	Filters were weighted before and after sampling to measure particle mass.	Sampling bias was not mentioned. Effect of temperature on artifacts was not included.	(39)
	Mining outdoor air	NA	QFF PUF	HPLC	$4.1 \times 10^{-4} – 1.9 \times 10^{-2}$	QFFs were ultrasonically extracted with n-hexane-DCM, while PUF plugs underwent extraction with Soxhlet, and both extracts were cleaned using liquid-solid chromatography.	Particle" properties were not studied. Sampling bias and effect of temperature on the bias were not included.	(40)

Urban outdoor air	PM_{10}	GFF PUF	GC/MSD	$4.7 \times 10^{-4} – 6.7 \times 10^{-3}$ (summer) $2.2 \times 10^{-3} – 6.6 \times 10^{-2}$ (winter)	PUF plugs and GFFs were Soxhlet extracted for 4 h and 10 h, respectively, and the concentrated extracts were analyzed.	Particle" properties were not studied. Sampling bias and effect of temperature on the bias were not included.	(41)
Urban outdoor air	4-6 0.9-1.2 0.4-0.45 0.13-0.17 ~0.05	Nano-MOUDI Al Foil	TD-GC/MS	1.5×10^{-3} 2.6×10^{-3} 8.9×10^{-4} 7.2×10^{-4} 3.8×10^{-4}	Sampling was conducted in different temperature. PAHs collected on Al foils were analyzed using in-injection port thermal desorption coupled with GC/MS.	Effect of temperature on GPP is not considered. Sampling bias was not documented.	(42)

	-Indoor cooking	>18	MOUDI	GC/MS	$4.1 \times 10^{-5} – 6.1 \times 10^{-4}$	Particle sample underwent three separate ultrasonic extractions, and each gaseous sample was subjected to Soxhlet extraction.	Although three particle sources were collected, the effect of composition on the partitioning was not studied. Effect of sampling bias was not considered.	(14)
		10-18			$6.6 \times 10^{-5} – 3.8 \times 10^{-4}$			
	-Indoor smoking	5.6-10	PUF		$4.7 \times 10^{-5} – 3.3 \times 10^{-4}$			
		3.2-5.6			$9.7 \times 10^{-5} – 4.1 \times 10^{-4}$			
	-Outdoor haze	1.8-3.2			$1.5 \times 10^{-4} – 6.3 \times 10^{-4}$			
		1-1.8			$2.5 \times 10^{-4} – 9.7 \times 10^{-4}$			
		0.56-1			$3.3 \times 10^{-4} – 1.1 \times 10^{-3}$			
		0.32-0.56			$3.9 \times 10^{-4} – 1.5 \times 10^{-3}$			
		0.18-0.32			$3.8 \times 10^{-4} – 1.6 \times 10^{-3}$			
		0.1-0.18			$4.7 \times 10^{-4} – 2.1 \times 10^{-3}$			
		0.056-0.1			$2.7 \times 10^{-4} – 1.4 \times 10^{-3}$			
BaP	Urban outdoor aerosol	PM_{10}	PTFE-coated GFF PUF	GC/MS	2.5×10^{-1} (summer) 6.3×10^{-1} (winter)	Filters were weighted before and after sampling to measure particle mass.	Sampling bias was not mentioned. Effect of temperature on artifacts was not included.	(39)

Mining outdoor air	NA	QFF PUF	HPLC	2.2×10^{-1} – 11.22	QFFs were ultrasonically extracted with n-hexane-DCM, while PUF plugs underwent extraction with Soxhlet, and both extracts were cleaned using liquid-solid chromatography.	Particle" properties were not studied. Sampling bias and effect of temperature on the bias were not included.	(40)
Urban outdoor air	4-6 0.9-1.2 0.4-0.45 0.13-0.17 ~0.05	Nano-MOUDI Al Foil	TD-GC/MS	4.78 8.51 2.81 2.29 1.17	Sampling was conducted in different temperature. PAHs collected on Al foils were analyzed using in-injection port thermal desorption coupled with GC/MS.	Effect of temperature on GPP is not considered. Sampling bias was not documented.	(42)

Urban outdoor air	NA	HVAS-QFF PUF	GC/MS	$5.9 \times 10^{-3} – 9.6 \times 10^{-1}$	Sampling was conducted in different temperature. HVAS, calibrated and operated at an average flowrate of 0.66 m^3 min^{-1} for 48 h	Effect of temperature on GPP is not considered. Sampling bias was not documented.	(43)

2.1.3 Equilibrium models to describe partitioning

The first equilibrium model for describing the partitioning was suggested by Junge (1977) based on adsorption approach (44), which was further developed by Pankow (1987), where the concept of particulate phase fraction φ was introduced (45):

$$\varphi = \frac{C_J \theta}{C_J \theta + P_L} \tag{2.3}$$

where C_J (Pa.cm) is determined by considering the heat released during desorption from the surface of particles, the heat required for vaporization of the compound, and the number of adsorption sites available on the particle θ ($cm^2_{surface}/cm^3_{air}$) represents the concentration of particle surface area, and P_L (Pa) corresponds to the vapor pressure of the sub-cooled liquid which depends on the air temperature.

Later, Harner and Bidleman et al. described the GPP coefficient ($K_{P\text{-}HB}$) as an absorption process and they assumed that the partitioning of SVOCs on particle (organic film covered the surface of particle) is resemble to partitioning of SVOCs into octanol (23)). Assuming the density of octanol is 820 kg m^{-3}, they derived an equation under equilibrium condition (Equation 2.4) as:

$$log\ K_{P-HB} = logK_{OA} + logf_{OM} - 11.91 \tag{2.4}$$

where K_{oa} is the octanol/air partition coefficient of the substance, and f_{OM} is the fraction of organic matter in the particle mass.

While these two models attempted to formulate the partitioning mechanism based on either adsorption (Equation 2.3) or absorption (Equation 2.4), others tried to consider the partitioning mechanism as a combination of both. Dachs and Eisenreich (2000) assumed that the elemental carbon (EC) is a criterion of the soot phase (corresponding to the adsorption process); therefore,

the Dachs-Eisenreich model of GPP coefficient ($K_{P\text{-}DE}$) adds the adsorption term to the absorption-based H-B model as (46):

$$K_{P-DE} = K_{P-HB} + K_{P-EC} \tag{2.5}$$

where $K_{p\text{-}EC}$ is the adsorption term and estimated by the following equation

$$K_{P-EC} = 10^{-12} f_{EC} K_{SA} \tag{2.6}$$

where f_{EC} represents the fraction of elemental carbon in particular matter (unitless), and K_{SA} is the soot-air partition coefficient (L/Kg).

Abraham (1993) studied the gas-particle partitioning of SVOCs at molecular level and developed poly-parameter linear free energy relationship (pp-LFER) model (47), which was then modified by Goss (2005) as follows (48):

$$logK_{P-L} = sS + aA + bB + vV + lL + c \tag{2.7}$$

where the uppercase letters represent SVOC descriptors that correspond to different types of phase-related interactions. S denotes the dipolarity/polarizability of the substance. The lowercase letters represent the complementary phase descriptors, and they are obtained through a multiple linear regression analysis. A and B describe hydrogen-bond acidity and hydrogen-bond basicity, respectively. V is the molar volume (McGowan volume), L is the logarithmic of hexadecane–air partition constant at 25 ˚C. These two descriptors are utilized to describe non-specific interactions, such as the energy associated with cavity formation and the energy arising from dispersive van der Waals interactions (49).

In a subsequent study, Gotz et al. introduced the pp-LFER model, describing both absorption and adsorption to aerosol particles, by which K_p can be calculated (50). This model was specifically designed to account for the complex, multi-phase nature of particulate matter. Subsequently, Shahpoury et al. considered carbon, $(NH_4)_2SO_4$, and NH_4Cl as components of the adsorbent in the adsorption process, and organic matter and organic polymers as the absorbent in the absorption process (51). The G/P partitioning quotient (considering the multiphase of particles), K_{P-mL}, expressed in units of μg/m³, can be calculated using the following equation:

$$K_{P-mL} = [\big(K_{EC} \times a_{EC} \times f_{EC} + K_{(NH_4)_2SO_4} \times a_{(NH_4)_2SO_4} \times f_{(NH_4)_2SO_4} + K_{NH_4Cl} \times a_{NH_4Cl} \times f_{NH_4Cl}\big) + \left(\frac{K_{DMSO}}{\rho_{DMSO}} \times f_{OM,A} + K_{PU} \times f_{OM,B}\right)] \times 10^{-6} \quad (2.8)$$

where K_{EC}, $K_{(NH_4)_2SO_4}$,K_{NH_4Cl} represent the target substance partitioning (adsorption) coefficients (mol m^{-2} $_{surface}$/mol m^{-3} $_{air}$) for elemental carbon/diesel soot, ammonium sulfate, and ammonium chloride, respectively. a_{EC}, $a_{(NH_4)_2SO_4}$, a_{NH_4Cl} denote the specific surface areas of the adsorbents (m^2 $_{surface}$/g $_{adsorbent}$), and f_{EC}, $f_{(NH_4)_2SO_4}$, f_{NH_4Cl} represent the mass fractions of these respective adsorbents within particulate matter ($g_{adsorbent}$/g $_{PM}$). K_{DMSO} (m^3 $_{air}$/m^3 $_{DMSO}$) and K_{PU} (m^3 $_{air}$/m^3 $_{PU}$) represent the substance partitioning (absorption) coefficients for the dimethyl sulfoxide-air and polyurethane-air systems, respectively. ρ_{DMSO} is the density of dimethyl sulfoxide. $f_{OM,A}$ and $f_{OM,B}$ are the mass fractions of absorbing phases ($g_{absorbent}$/g $_{PM}$). Here A corresponds to low to high molecular mass absorbent, including both water-soluble (WS) and organic-soluble (OS), organic matter (OM), and B corresponds to high molecular mass organic polymers absorbent (OP).

2.1.4 Steady-state models describing partitioning

Li et al. found that some equilibrium-based models cannot predict satisfactorily the results from the monitoring data in most cases for polybrominated diphenyl ethers (PBDEs) (26). They suggested that the GPP behavior of PBDEs follow a steady-state model. By considering dry and wet depositions of particles, they developed a model (L-M-Y model), and added a non-equilibrium term (logα), which is a function of octanol–air partition coefficient and temperature, model (Equation 2.4). In the L-M-Y model (Equation 2.9), equilibrium is a special case where logα equals to zero. The equilibrium and non-equilibrium states were distinguished by three zones: equilibrium domain (EQ domain), non-equilibrium domain (NE domain), and maximum partition domain (MP domain) based on values of K_{OA}.

$$logK_{P-LMY} = logK_{P-HB} + log\alpha \quad (2.9)$$

and logα is:

$$log\alpha = -log(1 + 4.18 \times 10^{-11} f_{OM} K_{OA}) \quad (2.10)$$

2.2 Factors that affect GPP

Primary particles released from geogenic, anthropogenic, and biogenic origins have different characters. The characteristics of secondary particles are largely influenced by the way they are created and the specific compounds that contribute to their formation. Primary inorganic particles play an important role in shaping secondary inorganic-rich particles by regulating condensation, coagulation and nucleation processes (52,53). Secondary organic aerosol (SOA or secondary organic-rich particles) generates from a series of complex oxidation reactions of VOCs/SVOCs (54,55). Secondary particles from different origins have different properties such as composition,

morphology, and particle size. These properties can influence the GPP (56). In the following, the impact of these properties on GPP will be discussed.

2.2.1 Impact of composition

Particle composition is an important factor in regulating the interaction of particle and SVOCs, and equilibrium state of partitioning of SVOCs on the surface of particles (57). In fact, it is a key factor in partitioning behavior (absorption and adsorption processes) of a SVOC (17). Andersen et al. compared PCB-particle phase concentrations in a PCB contaminated room for particulate matter generated by burning candles and cigarettes (58)). They showed that an increase in cigarette particle concentration resulted in an increase in indoor air particle concentration of PCBs. On the other hand, increase in candle burning particles did not result in such an increase. This indicates that different types of organic sources composing particles can influence the amount of PCBs being absorbed to the particle. Bi et al. assembled a chamber in which two types of dust, Arizona dust, which is almost composed of inorganic matters, and a dust sample from a vacuum cleaner bag containing 32% organic carbon, were in direct contact with two sources of DEHP and DnBP (a vinyl floor) (59). The concentrations of both DEHP and DnBP in house dust were almost three times greater than Arizona test dust after 20 days contact to the vinyl floor, indicating carbonaceous dust had a better interaction with these two types of phthalates.

Kondo et al. developed a setup in which three different particles; one Japanese test aerosol called Kanto Loam (KL, a mix of inorganic compounds), and two atomizer generated particles (carbon black (CB) and silica), were exposed to DEHP gaseous in a 60 L aging chamber (60). For collecting samples, stream was divided into two passes with a valve. Gas-phase DEHP was collected on a Tenax-TA tube and particle-phase DEHP was collected on a quartz filter which the gaseous DEHP was removed before by a diffusion tube. They reported that the adsorption of DEHP

on silica is higher than KL and CB particles and suggested that the difference was due to an assumption that these particles are spherical, and the surface area concentration of each particle was calculated based on spherical morphology.

Wu et al. used a stainless chamber to study gas-particle partitioning of DEHP to one inorganic (ammonium sulfate) and two organic (oleic and squalene) airborne particles (61). They measured the partition coefficient of DEHP (K_p) for these particles, and they showed that the value of K_p for organic particles are much higher than ammonium sulfate particle (Table 2.2), suggesting that gaseous DEHP can interact with organic particles in an absorption mechanism.

2.2.2 Impact of morphology

The morphology of particles plays an important role in regulating the dynamic of gas-particle interaction by determining the gas-particle equilibrium timescale. In fact, it has a direct effect on the mass transfer from air to the surface (external mass transfer process) and diffusion into and out of the particle (internal mass transfer process). Liu et al. considered the structures of airborne particles into four spherical nonporous and porous morphologies covered by a homogenous liquid-like organic layer to compare the external mass transfer and the internal mass transfer processes (62). They developed a dimensionless mass transfer model which is a function of two dimensionless factors, Bi_m/K_{part} and f_v where the former is an overall coefficient comprising mass transfer coefficient around particles, intraparticle diffusion coefficient, gas-particle partition coefficient and particle size, and Bi_m is the Biot number ($Bi_m = \frac{v_t R_2}{D_{sp}}$ where v_t (m/s) is the gas/particle mass transfer coefficient, R_2 (m) is the radial distance of permeable outer layer of particle, and D_{sp} (m^2/s) is the internal diffusion coefficient). The latter (f_v) is the volumetric fraction of permeable part of particles. By setting critical values based on Bi_m/K_{part} and f_v graph, they calculated that internal resistance (diffusion in and out of particles) is insignificant. Their finding

was in contrast with the Strommen and Kamens's (1997) findings (63) in which they showed that for soot particles from wood and diesel combustion sources the adsorption and/or tortuosity in the inner layer are more significant than the outer layer.

Particulate matters possess different morphologies (Figure 2.1), and their structure can highly affect the interaction dynamic of SVOCs (64). The specific ways in which particle morphology affects these interactions can vary based on factors such as particle surface area, porosity, and shape. For example, porous particles can absorb SVOCs into their internal structure influencing the overall capacity of the particles to retain these compounds. The porous nature of certain particle morphologies can enhance the absorption of SVOCs.

For having a comparable result in counting non-spherical particles, the concept of an equivalent diameter has been defined. Although this concept is valuable in particle filtration and health assessment filed, it can be a source of bias in understanding the gas-particle partitioning processes, for instance the effect of particle's porosity is neglected. Therefore, it is vitally important to study the equilibrium timescale of non-spherical particles, particularly for quasi-fractal particles for which the gyration diameter and the fractal dimension of aggregates or agglomerates have been introduced to describe their equivalent diameter and their compactness (65).

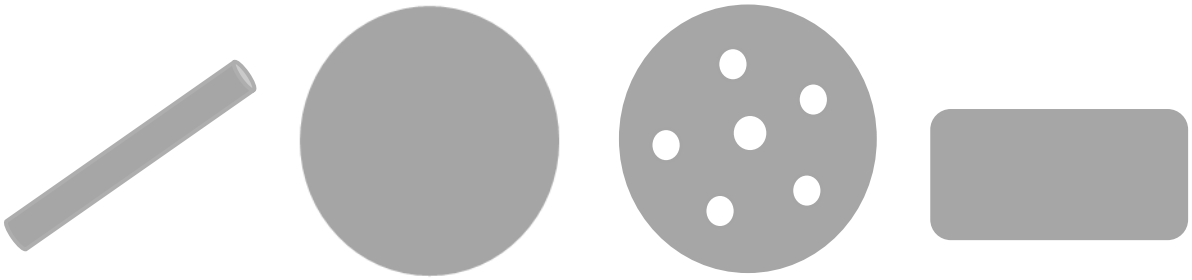

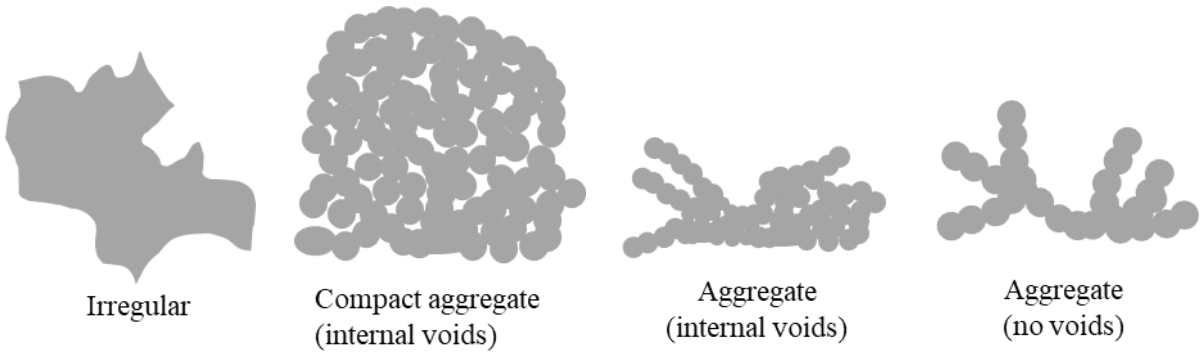

Figure 2.1.Different particle morphology adopted from DeCarlo et al. and Li et al. (58,59).

2.2.3 Impact of particle size

Particle size distribution is an important factor that can have an impact on the gas particle partitioning and consequently have a direct effect on the partitioning coefficient. Besides, particle size can provide information how long the sorbed SVOC is airborne.

Many studies (66–68) have indicated that low molecular weight PAHs (LMW) emitted from combustion sources are mainly bounded with fine and coarse particles, whereas high molecular weight (HMW) PAHs are mainly sorbed to fine particles. One explanation provided by these studies is the co-emission of specific PAHs and fine particles. Allen et al. proposed two hypothesises to explain why HMW PAHs are more dominantly associated with fine particles (69): 1) low molecular weigh PAHs tend to partition to the coarse mode through volatilization from fine particles and condensation onto coarse particles while high molecular weight PAHs exhibit lower fluxes through volatilization and condensation. Consequently, they tend to persist on the fine particles with which they were originally emitted. 2) Variations in chemical affinities exist among individual PAHs and particles of different sizes.

As to non-combustion-related sources, Mandalakis et al. reported the same trend for PBDEs (70). Low molecular weight compounds, such as BDE 17, were associated with coarse particles, whereas heavier compounds were mainly adsorbed/absorbed to the finer particle. Hu et al. divided

particles into 11 stages according to their size by using size-segregated samples (MOUDI). Although they did not consider sampling bias (71), this method is a proper approach to calculate gas-particle partitioning coefficient over a range of particle size distribution. An interesting outcome was that the fraction of organic matter was higher in finer particles. Moreover, for most of the BDEs the size-segregated particles graph showed a unimodal distribution with a peak concentration in 0.56-1 μm. Later, Wang et al. used the same method and reported that Log K_p has a peak value in the size fraction of 0.1-0.32 μm for high molecular weight PAHs (14). As to the behaviour of indoor OPEs and PAEs, they revealed that size-resolved particle partitioning exhibited a bimodal distribution, and these groups were dominant in extremely fine particles (<100 nm) and coarse particles (>1 μm). They argued that the variations in K_p values of a compound for different particle size fraction stem from different dominant partition mechanisms (absorption, adsorption, or both) associated with various particle sizes; moreover, it was noted that extremely fine particles due to their large specific area have higher tendency to absorb/adsorb volatilized OPEs and PAEs on their surface, while those released through mechanical wearing and weathering are initially distributed in coarse particles.

2.2.4 Impact of humidity and temperature

Increased temperature promotes emissions of SVOC from building materials resulting in higher gas-phase concentrations. For example, increasing temperature leads to an increase in gas-phase PAEs in indoor spaces (72–74). Clausen et al. conducted an experiment test on one type of polyvinyl chloride (PVC) flooring (source of phthalates) using a Field and Laboratory Emission Cell (FLEC) chamber to study the effect of temperature on PAEs emission (72). They illustrated that by increasing temperature from 23 °C to 61°C, DEHP concentration increases almost 200-fold from 0.9 $\mu g.m^{-3}$ to 198 $\mu g.m^{-3}$ due to the higher DEHP emission rate at higher temperature.

Analyzing the available experimental data in the literature, Wei et al. showed a strong correlation between temperature and K_p values (16). This study needs further validation as the correlation assumed that the interaction is governed by absorption process and that the absorbent (particle matter) has a porous structure.

Chen et al. generated three different concentrations of gaseous phthalates using a porous media under both uncontrolled and controlled temperature conditions, respectively (75). They showed that controlling temperature condition performed better in generating phthalates with respect to stability and quick response. Zhou et al. investigated the impact of both temperature and humidity on the gas-particle partitioning (76). They showed that although an increase in temperature resulted in an increase in phthalate concentration in both gas and particle phases, temperature had inverse relationship with K_p. Results suggested that humidity had negligible effect on the gas-particle partition phthalate and no effect on the phthalate concentrations in gas-phase, albeit it increased the particle-phase concentration. They concluded that the effect of humidity on gas-particle partitioning did not follow any specific pattern.

Bi et al. suggested that relative humidity can affect phthalate partitioning of inorganic due to an adsorption process which dominates the air/dust partitioning (59). Moreover, they found that relative humidity has an inverse relationship with DnBP partitioning on Arizona test dust (ISO 12103-1, A3 medium test dust, Powder Technology Inc), but not with DEHP. The inconsistent findings reported by different group suggests that the effect of humidity on SVOCs sorption to particulate matter and dust is still not clear.

Table 2.3. Studies on implementing models (both equilibrium and steady state) on measured data available in the state-of-the-art.

Compounds	Equations	Advantage and Remarks	Limitation	Reference
PAHs	Eq (2.3) Eq (2.4) Eq (2.5)	-Soot-air models tend to predict partitioning better. -The fraction of soot has a significant impact on middle molecular weights PAHs partitioning.	Particle characterises such as fraction of elemental carbon and organic matter, particle size, and phase of particle, were not documented. Sampling bias is not considered.	(18)
PAHs	Eq (2.8)	Consider the effect of breakthrough. First study to classifying particle composition. Results showed LMW PAHs tended to partition on particle in both absorption and adsorption, while heavier compounds partition mostly in absorption process.	Effect of particle size on partitioning model was not considered. An enhanced understanding of organic matter composition is essential. Functionalizing organic matter phase-state in model is needed. ADR was set by a region of ±1 log unit deviation.	(51)
PAHs	Eq (2.3) Eq (2.4) Eq (2.5)	Adsorption and absorption models tended to underestimate the particle-bound fraction for most PAHs. The dual aerosol-air/soot-air model provided a more accurate.	Breakthrough and adsorption on particle filter was not involved. Particle size was formulated in models. Effect of temperature on partitioning was not documented.	(77)
PAEs	Eq (2.7)	The pp-LFER model predicted the partitioning reliably.	Data was provided by literature. Particles assumed to be homogenous. Particle properties	(20)

			was not considered. Sampling bias was not involved.	
PAHs	Eq (2.4) Eq (2.5) Eq (2.8)	The H-B and D-E models showed a better prediction in compare with the L-M-Y models for 5-rings PAHs.	Particle properties were not documented. Sampling bias was not considered.	(78)
PBDEs	Eq (2.3) Eq (2.4) Eq (2.5) Eq (2.7) Eq (2.8) Eq (2.9)	In EQ domain (Log K_{OA}<11.4) all models tended to predict well. When Log K_{OA}>12.5 (MP domain) the L-M-Y model performed well in predicting the partitioning coefficient.	The sampling bias and effect of temperature on partitioning were not considered. ADR was set to a deviation of ±1 log unit. Particle properties was not documented.	(79)
PAHs	Eq (2.3) Eq (2.4) Eq (2.5)	Three sources of PAHs, involving condensate, diesel, and heavy oil, were studied. Sampling bias was considered by installing three PUF in series.	Although three different sources were selected, particle properties were not characterized. The effect of particle age should have been involved.	(80)
PCBs	Eq (2.3) Eq (2.4) Eq (2.5) Eq (2.7) Eq (2.8) Eq (2.9)	The effect of particle size was considered in predicting Log K_p. The performance of L-M-Y model was much better in MP domain. However, the ratio of predicted values to measured one was 1.25 ± 1.44.	The sampling bias and effect of temperature on partitioning were not considered. ADR was set to a deviation of ±1 log unit. Particle composition was not documented.	(81)
PBDEs, PAEs, PAHs, OPEs,	Eq (2.4) Eq (2.9)	72.0% of mean data of steady model were within the acceptable data range (ADR) while 56.0% were within the	For calculating GPP from literatures, temperature and TSP values were set based on assumption. The percentage of	(82)

FRs, OCPs, PCBs, parabens, and phenols		ADR of equilibrium model. Notably, in the MP domain, 83.3% aligned with the ADR of steady model, contrasting sharply with only 16.7% within the ADR of log $K_{P\text{-}HB}$.	organic matter on particle assumed to be 0.4. ADR was set by a region of ±1 log unit deviation. Models tended to underestimate the partitioning for compounds with lower K_{OA}.	

2.3 Discussion

Table 2.3 provides a summery of studies on implementing gas-particle SVOCs partitioning models (section 2.1). As to PAHs, Wang et al. and Pratt et al. found that the adsorption/absorption models (octanol-air/soot-air model Equation 2.5) performed better in predicting K_p values in comparison with single factor sorption models (either adsorption or absorption models, Equation 2.3 or Equation 2.4) (18,77). As to PCBs, Qiao et al. reveled that the pp-LFER underestimated the log K_p (only 7% of data points in acceptable data range (ADR)) when log K_{OA}<9.5. They came to almost the same conclusion that in MP domain (when log K_{OA} > 11.4) L-M-Y model performed better than equilibrium models (H-B and D-E models) (81). These studies defined ADR as: $-1 \leq \Delta \log K_P \leq 1$ while there is no valid standard for setting these criteria. Further studies are needed to set a criterion for ADR. Although the percentage of organic matter on particles is used as a determining factor in absorption process, non of the studies documented it.

The process of sampling indoor air can introduce artifacts that may affect the partitioning behavior of SVOCs between gas and particle phases. These artifacts can lead to discrepancies between predicted and observed partitioning behavior. Bias occurs depending on several parameters such as physiochemical properties of compounds, the concentration of particles, the distribution of particle sizes, sampling velocity, and sampling time (83) (84). Therefore, the effect of the temperature on sampling and sample integrity should be considered when it comes to comparing

data. Another important factor is degradation of the compounds on the sampler due to presence of reactive gases (85,86). For instance, Pehnec et al. found a notable negative correlation between concentrations of PAHs and ozone concentrations (87). It was reported that the influence of ozone is more prominent in PAHs with higher molecular weights. Hence, to avoid bias in sampling and having credential data to compare, it is of utmost importance to set and report the sampling condition.

As mentioned, all models (with exception of pp-LFER model) used either P_L or K_{OA} as a correlating parameter for K_P. One of the problems of using P_L is finding a correct and accurate value of P_L; however, none of the studies measured P_L in field. It should be noted that P_L is a function of temperature. As for K_{OA}, although this factor is useful for understanding the partitioning of compounds between air and lipids, it may not correspond to the partitioning behavior of SVOCs between gas and particle phases. For example, DEHP and BaP possess almost the same value of log K_{OA} (Table 2.1), albeit they have different values of K_p (Table 2.2). This means that the activity of compounds in octanol phase may not be analogous to their activity in organic material phase. Partitioning of (SVOCs) in indoor environment can be affected by a range of factors including particle size, composition, and surface characteristics, aspects that are not fully accounted for by octanol. Therefore, the difference in K_p values predicted by models and experiments calls for more diligence in both refining models (by considering different particle range sizes, particle compositions, etc.) and improving experiment designs. Potential bias in experimental settings and especially in sampling must be dealt with.

2.4 Summary

In this study, models describing gas-particle partition (both equilibrium models, containing adsorption, absorption, and adsorption/absorption models and steady state models) and important

factors that affect SVOCs gas-particle partitioning in indoor environments were reviewed. Due to variety of exhibited by particles and diverse behaviour of SVOCs even within the same group (e.g., DnBP and DEHP from phthalates), the gas-particle partitioning of SVOCs needs a characterization of both particles and SVOCs properties. Particle properties can influence the partitioning process and the time to reach equilibrium; it is vitally important to report particle size distribution and particle composition during SVOCs samples. Particle composition, for example, can provide information on what process will take place. Although previous studies showed that SVOCs tended to partition on finer particle, more studies are needed to distinguish the effect of composition as the particle possesses different composition in different size (88). Moreover, for having a realistic knowledge of equilibrium timescale, it is vitally important to study and consider the effect of particle morphology on K_p values, particularly aggregated particles for which the gyration diameter and the fractal dimension have been introduced.

Furthermore, K_p values calculated from the literature were compared for selected compounds. This comparison is challenging and may introduce bias. One of the reasons is that particles were collected from different sources, leading to variations in selected SVOC behavior mechanisms toward particles. Another challenge arises from different sampling conditions, which can introduce bias in particle-phase SVOCs concentration and in the calculation of K_p. Future research should focus on developing a standardized method to better characterize the influential parameters, harmonize sampling and analytical methods. For example, particles should be in monodisperse mode from which one can analyze the effect of particles size and formulate it in models; a long Differential Mobility Analyzer (DMA) may be used in this case as an option.

3 Methodology

3.1 Chemicals

Four phthalates including Diethyl phthalate (DEP), di-n-butyl phthalate (DnBP), benzybutyl phthalate (BzBP), and di-2-ethylhexyl phthalate (DEHP), covering wide range of vapor pressures, were selected. All chemicals were analytical grade and standards and were purchased from Sigma-Aldrich. Methanol was HPLC-grade and was acquired from Fisher Scientific. Physicochemical properties of selected phthalates are presented in Table 3.1.

Table 3.1. Physiochemical properties of targeted phthalates.

Phthalate	MW (g/mol)	Vapor pressure (P^o, Pa)	Structure	Ref
DEP (Diethyl phthalate)	222.24	1.8E-01	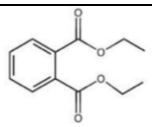	(22,89)
DnBP (Di-n-butyl phthalates	278.34	4.6E-02	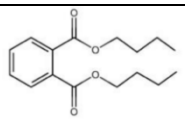	(22,25)
BzBP (Benzyl butyl phthalate)	312.36	4.9E-03	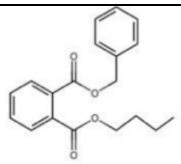	(22,25)
DEHP (Di-2-ethylhexyl phthalate)	390.55	2.3E-04	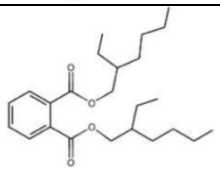	(22,25)

3.2 Generation system

The generation system consists of three different dynamic generators: particle generation, light and medium phthalate generation (DEP and DnBP), and heavy phthalate generation (BzBP and DEHP).

3.2.1 Particle generation

Particulate matter is generated by using a collision-type atomizer, model 3076 Constant Output Atomizer (TSI) (Figure 3.1), that can atomize most solutions or suspensions. The solute concentration dictates the particle size of the aerosol. For the first objective, sodium chloride (NaCl) particles were generated from a 300 mg/L NaCl solution in distilled water using the atomizer. As to the second objective, NaCl particles in the range of 300-375 nm, 579-721 nm and 897-1117 nm were generated by nebulizing (2.5 L/min) the aqueous NaCl solution of 350 mg/L, 500 mg/L and 600 mg/L, respectively. Generated particles with an airflow of 2.5 L/min, were then passed through a drying system with a pack of anhydrous silica gel to remove humidity from the airborne NaCl particles. For the third objective, the solution of 350 mg/L was selected for comparison purposes. As the preliminary results showed that the outlet mass concentration (TSP) of particles with mean diameter of 337 nm (about 450 $\mu g/m^3$) and 650 nm (about 567 $\mu g/m^3$) were higher than that of 1007 nm particles, the outlet for these particles were extracted by flow of 0.4 L/min and 1 L/min, respectively, and then diluted with clean air at the same airflow rate to achieve the desired TSP between 313 to 375 $\mu g/m^3$ after the mixing chamber.

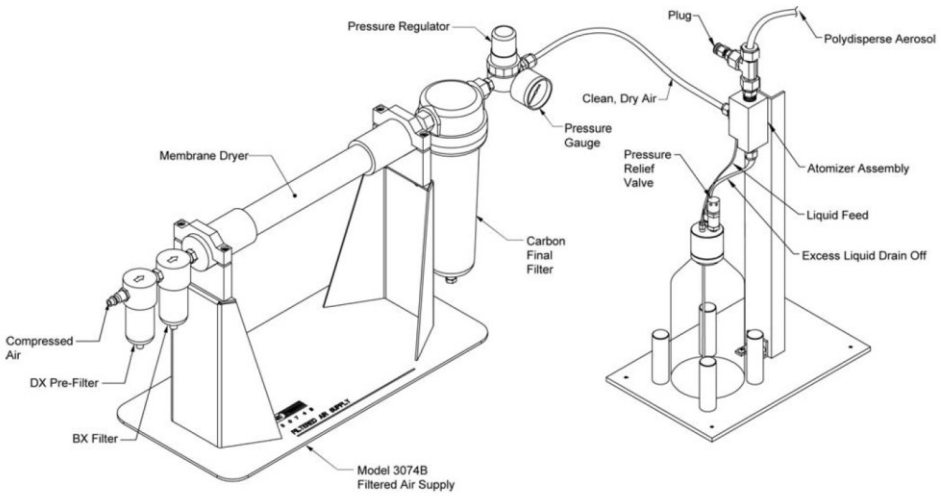

Figure 3.1. Model 3076 Atomizer in the Recirculation Mode

3.2.2 Phthalates generation

The generator system for phthalate concentration had three different setups: 1) light phthalate generator for DEP (Figure 3.2 a), 2) moderate weight phthalate generator for DnBP (Figure 3.2 b), and 3) heavy weight phthalate generator for DEHP and BzBP (Figure 3.2 c). The generation system for all setups used an embedded glass fiber method. Briefly, 15 ml of selected compound was carefully poured onto a fibrous glass, and 24 hours was set to let the compound fully disperse in the media. Then the embedded media was inserted to a stainless-steel tube (for heavy phthalates) or a glass tube (for light/moderate phthalates). Compressed air flow was regulated to 500 ml/min for all cases using a mass flow controller (MFC). For the DEP generator (Figure 3.2 a), due to the high concentrations generated, the flow at outlet was diluted by extracting 20 ml/min from the generator, using a rotameter to adjust the flow, and mixing with 480 ml/min of clean air. For heavy phthalate, a hot plate was used to heat the stainless-steel tube to accelerate the emission rate to achieve desirable concentrations at the outlet (Figure 3.2 c). To attain a similar concentration as DEP and DnBP, the temperature on the hot plate was set to 33 ºC and 57 ºC for BzBP and DEHP,

respectively. The temperature and humidity at the outlet of the chamber were monitored, using a sensor (Rotronic- HP32 HygroPalm Digital), and kept at 20 ± 1.5 ºC, and at 15 ± 7 %, respectively.

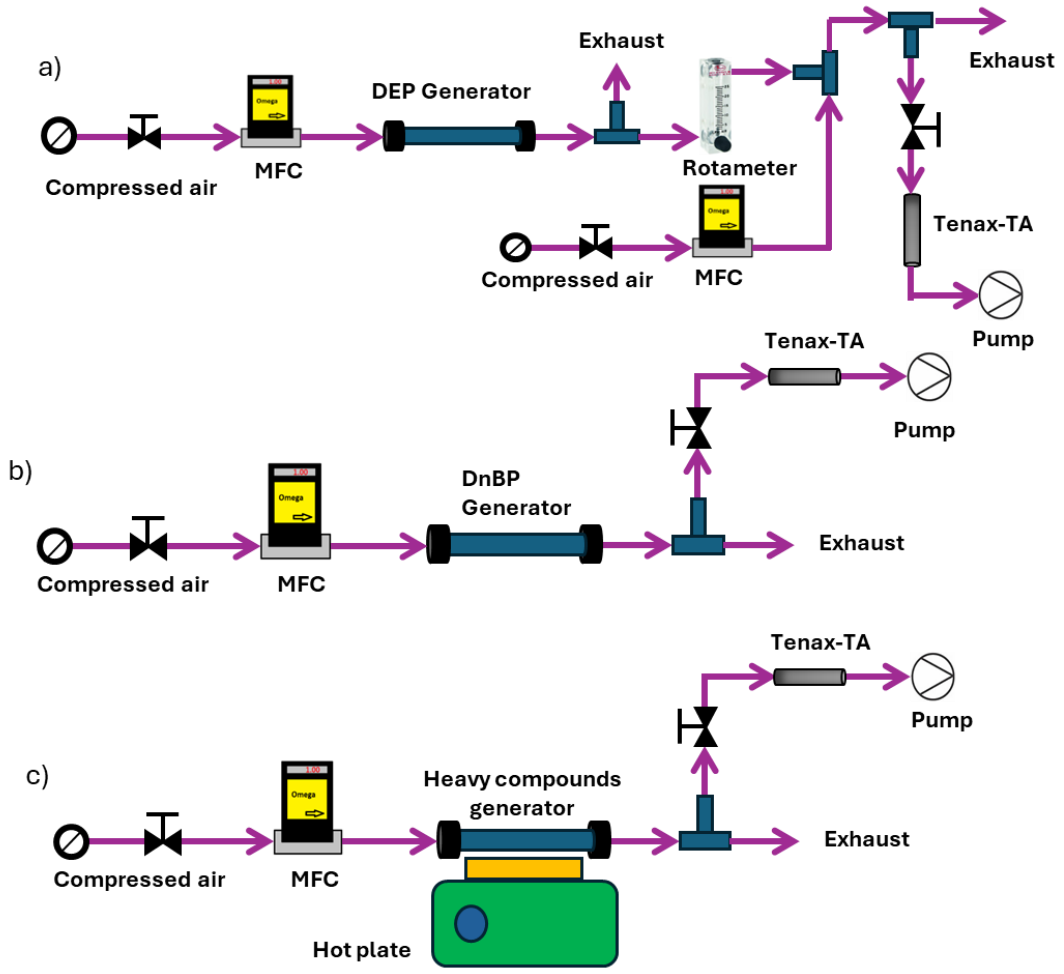

Figure 3.2. Schematic of all types of gaseous phthalates generators along with their collection system; a) embedded light phthalate (DEP) with a dilution system, b) moderate phthalate (DnBP) generator, and c) heavy compounds with a hot plate.

3.2.2.1 Generation of phthalate mixture

For assessing the effect of phthalates' competition towards adsorbing to the particle, a mixture of phthalates consisting of DnBP and BzBP were introduced to the mixing chamber. In this

experiment, gas phase DnBP and BzBP were generated separately following the same generation setup as the previous section; however, the airflow for each phthalate concentration generator was set to 250 ml/min, to a total of 500 ml/min for mixed phthalates. Particles were generated from 600 mg/L of NaCl in water as described earlier. Then after, particles and two phthalates were co-introduced to the mixing chamber.

3.3 Mixing chamber

After generation, the particles and selected phthalate were co-injected (co-introduced) into a rectangular mixing chamber (Figure 3.3) with a volume of about 51 liters (42.5 cm × 40 cm × 30 cm) and having of 5 walls of stainless-steel and one wall of glass (90,91). The temperature at the outlet of the chamber was monitored and kept at 20 ± 1.5 ºC. Losses of particles and phthalates for each configuration were measured by taking samples from upstream and downstream of the mixing chamber and found to be minimal (Table 3.2).

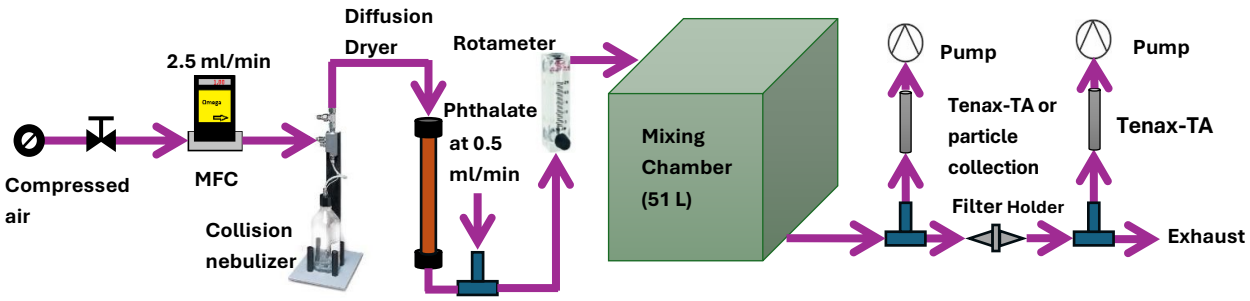

Figure 3.3. Schematic of the K_p measurement setup consisting of the particulate generator system, and the mixing chamber with the collection pathway for total phthalate concentration and gas-phase concentration.

Table 3.2. Phthalate and particle losses in each configuration.

Configuration	DEP	DnBP	BzBP	DEHP	Particles
DEP/Particle	1-2.7 %	-	-	-	1.5-4.8%
DnBP/Particle	-	1.4-3.9 %	-	-	1.4-5.1%
BzBP/Particle	-	-	5.1-7.9 %	-	2.3-5.8%
DEHP/Particle	-	-	-	11.2-15.4%	2.9-6.9%
Mixture/Particle		2.5-6.3%	5.3-8.1%		2.7-6.7%

3.4 Limitation of the Experimental system

The mixing chamber and the experimental system provide a highly controlled environment and enables isolation of key parameters; however, several limitations should be acknowledged. First, wall sorption and re-emission may lead to misestimate in measuring phthalate gas-phase and particle-phase concentrations, particularly for lower-volatility phthalates. Second, temperature and humidity were maintained near indoor conditions but not varied (for isolating the effect of other factors such as particle size); therefore, the effect of indoor air conditions (temperature and humidity) is not fully addressed. Third, the indoor air contains of a complex mixture of particle composition (e.g. organic particles, biogenic particles, suspended dust) which the simplified particle system (pure NaCl aerosols) and single-pass configuration cannot represent such complexity. These limitations do not affect the internal validity of the mechanistic findings because NaCl was chosen for the purpose of isolating adsorption from absorption partitioning, but they indicate that future work should incorporate dynamic indoor factors and more realistic particulate matrices.

3.5 Collection method

3.5.1 Phthalate collection

Sample was collected at two stages: 1) generator's outlet concentration validation (Figure 3.2), 2) K_p value measurement (Figure 3.3). For the first stage, samples were collected at the outlet of the generators. For the second stage, all samples were collected after mixing chamber. For calculating K_p values, the collection pathway was separated into two passes by installing a PTFE membrane (1.0 μm pore size, diameter 25 mm, Fluoropore): one for collecting gas-phase phthalate (downstream of filter) and the other for collecting total airborne phthalate (upstream of filter). In each sample, preconditioned Tenax-TA tube was used to collect air samples from either downstream of phthalate generator or downstream of mixing chamber. To minimize the sorption area along the sampling path, the sorbent was attached as close as possible to the outlets. A gas sampling pump was used to collect generated pollutants at rate of 50 mL/min. The sampling period was 10 min, and 60 min for the first stage, and the second stage, respectively.

Figure 3.4. Model 3330 Optical Particle Sizer Spectrometer.

3.5.2 Particle collection

Particle matter counted through an Optical Particle Sizer (OPS) Spectrometers (Model 3330, TSI). The Model 3330 OPS spectrometer, depicted in Figure 3.4, is a high-performance particle

spectrometer designed to measure aerosol optical diameter. It delivers precise count size distributions for particles with optical diameters ranging from 0.3 to 10 micrometers. The OPS 3330 operates based on the principle of optical scattering from individual particles. Particles are illuminated using a laser beam shaped into a thin sheath and focused below the inlet nozzle. As particles traverse through this light sheath, they scatter light in the form of pulses, which are then counted and sized simultaneously. The concentration measured by the OPS is highly sensitive to the flow rate, thus the flow is rigorously controlled to 1.0 L/min with an accuracy of ± 5%.

3.6 Phthalate analysis

The collected gaseous phthalates on the Tenax-TA tubes were released from the sorbent bed using an automated thermal desorption system (TurboMatrix 650 TD, PerkinElmer). Thereafter, gaseous phthalates were introduced to the gas chromatograph/mass spectrometer (Agilent 6890/5975b GC/MS). The calibration of the GC/MS was conducted using test samples that covered the expected concentration range for all phthalates. The resulting calibration curve spanned from 5 to 200 ng/tube using reference points at 5, 20, 50, 100, and 200 ng/tube. Serial dilution in methanol produced calibration solutions that were then injected into the sorbent tubes in liquid form. A blank sorbent tube was used to check for background contamination before each experiment. For heavy compounds like DEHP, after each run a cleaning method was used to flush out any residual chemical. The GC column used was an HP-5MS UI (30 m long, 0.25 mm I.D., and 0.25 μm film thickness). The GC oven temperature program was set with an initial temperature of 40 °C, held for 5 minutes, followed by a ramp at 10 °C/min up to 300 °C, which was then held for 8.5 minutes. The transfer line connecting the GC to the MS was maintained at 280 °C (536 °F). The mass spectrometer was operated in positive electron ionization mode and set to full scan mode with a mass range of 30-400 amu.

3.7 Uncertainty and Repeatability

To avoid uncertainty in measured particle-gas partitioning coefficients (K_p), all experiments were performed three times under identical operating conditions (such as same sampling flow and time, same temperature etc.). This allows quantification of experimental variability due to sampling, analytical detection, and flow control stability. The relative standard deviations (RSD) of gas-phase and particle-phase concentrations remained within acceptable ranges (< 5%), indicating reliability of the reported K_p values and supporting their use for model validation.

3.8 Equations to describe particle-gas partitioning coefficients

By measuring particle-phase concentration C_p (μg/m^3), gas-phase concentration C_g (μg/m^3) of a compound, and total suspended particle (TSP) mass concentration (μg/m^3), the particle-gas partitioning coefficient (K_p, m^3/μg) was experimentally calculated using Equation 2.1. For model comparison purposes and to be consistent with previous studies we assumed C_J = 17.2 Pa.cm (the constant value).

4 Influence of Residence Time on the Particle-Gas Partitioning of Phthalates onto Airborne Inorganic Particle

Given the critical role of indoor air quality in human health due to prolonged occupancy time in enclosed environments, understanding the behavior of air pollutants is of paramount importance. Numerous compounds have been introduced into daily life through modern consumer products, many of which contain SVOCs to enhance their functionality (92–94). Some of these compounds can have negative health effects (95–97). Phthalate esters (PAEs), for example, have been widely used in products such as cosmetics, plastics, and medical devices (98,99). Since these compounds are typically not chemically bound to the materials, they can gradually emit into air, contributing to their ubiquitous presence in indoor environments (100). Due to their low vapor pressure, SVOCs readily partition onto various surfaces, allowing them to persist in indoor environments long after their primary sources have been removed (101,102).

Interactions between SVOCs and airborne particulate matter (PM) are referred to as particle-gas partitioning in indoor air quality studies (8,103–105). This results in increased bioavailability of SVOCs due to the omnipresence of PM and resultant inhalation exposure routes. In addition, previous modeling and experimental studies showed that the presence of PM in indoor air leads to an increase in total concentration of airborne SVOCs (sum of gas-phase and particle-phase concentrations) (106,107). Therefore, examining particle/gas partitioning is key to understanding SVOCs behaviour in indoor air, including their fate, transport, and health impacts (108).

The particle/gas partition coefficient (K_p), which determines the relative concentration of SVOCs in the particle phase, can be estimated using various models (26,51,109,110). To validate these results, many researchers have conducted studies comparing models with measured data mostly

from atmospheric studies (111–113). However, many of these studies are subject to bias such as artifacts and breakthrough due to the challenges posed by low vapor pressure of SVOCs as well as variations in data collection methods and environmental conditions (22, 23). Many factors can affect the partitioning processes, including particle properties, physicochemical properties of the targeted SVOC, and environmental conditions (7). In measuring K_p values for phthalates, as an example, Huang et al. (36) mentioned K_p exhibits varying values according to seasons. Wang et al. (14) revealed K_p values are particle size dependent. Another issue in estimating K_p is that most models have assumed an equilibrium state in SVOCs particle/gas interaction. However, Weschler and Nazaroff showed that depending on the particle size and octanol-air partition coefficient of the targeted SVOC, equilibration time scale can be prolonged for more than 10 h (far more than the residence time of pollutants indoors) (25). The AER can also affect SVOCs mass transfer from their sources (115,116). Clausen et al. showed that an increase in AER led to a decrease in indoor bis(2-ethylhexyl)phthalate (DEHP) concentrations, albeit along with an increase in emission rate from building materials (117).

Despite advancements in modeling, very little experimental research in this area has been conducted. Benning et al. (118) were the pioneers in measuring K_p value for DEHP toward ammonium sulfate particles, although their main objective was to characterize the effect of airborne particles on DEHP emission from a real source. Later, Wu et al. (61) measured K_p for DEHP and reported it is an order of magnitude higher value for organic particles in comparison with inorganic particles. These were the first study to examine the behaviour of SVOCs under different particle properties; however, the effect of type of particle on K_p values cannot be thoroughly distinguished as the size of different particles were not comparable and isolated. Zhou

et al. (76) investigated the effect of temperature and humidity on K_p values for PAEs. They showed that temperature has a strong negative correlation with K_p, but humidity has no obvious effect.

Given the significant role of ventilation rate (or AER) in regulating indoor SVOC behavior, this study aims to investigate the effect of AER (residence time) on particle/gas partitioning through a novel experimental approach. By utilizing a rapid gaseous phthalate generator and a mixing chamber to introduce generated particulate matter (NaCl) with the target phthalate, airflow rates can be adjusted to simulate real indoor air conditions. DnBP and diethyl phthalate DEP were selected because they had been detected at highest concentrations in Canadian nail salons (119), and had the highest mean concentrations in settled dust and in the air in both European residential and educational buildings (120).

4.1 Methodology

The following steps were taken for experimentally calculating the K_p values. Gaseous DEP and DnBP were generated from the embedded compound in fibrous glass media by driving 500 ml/min compressed air. Due to high concentration of DEP, its outlet concentration was diluted. In parallel, generated particles were co-injected with single phthalate into the mixing chamber. The combined airstream flow was set at 3 L/min, 2 L/min, and 1.5 L/min corresponding to a residence time of 17 min, 25 min, and 34 min, respectively. Experimental measurements were used to correct particle losses and phthalates losses caused by deposition and coagulation within the chamber. For airflows of 3 L/min, 2 L/min, and 1.5 L/min, the measured TSP, DnBP, and DEP mass losses (after 240th hour) ranged from 1% to 5%, 1% to 3.4%, and 1% to 2.7%, respectively. Moreover, the DnBP and DEP sorption to filter holder and the filter were at range of 4.1% to 7.6% and 2.2 % to 6.3%, respectively.

4.2 Results

4.2.1 Generating gaseous phthalates

Figure 4.1 illustrates the stability of the DnBP and DEP generation system in a 10-day period. The results show the generation system possesses three distinct phases: an initial burst, a fluctuating transition period, and the steady state period. The final concentration depicts that the system reached a dynamic equilibrium after the120th hour with an outlet concentration of 157.6 ± 5.7 µg/m^3. The initial outlet concentration of DEP system starts at high level (about 8000 µg/m^3), likely due to rapid volatilization from the media. After five hours, there are oscillations in the system, a more pronounced fluctuation in comparison with DnBP. Possible causes might be due to its higher vapor pressure, temporary adsorption/desorption within the system, and non-uniform release of DEP from the fibrous media. However, the DEP concentration stabilizes faster after the 50th hour and at a higher level of concentration (3578.2 ± 52.2 µg/m^3) than DnBP.

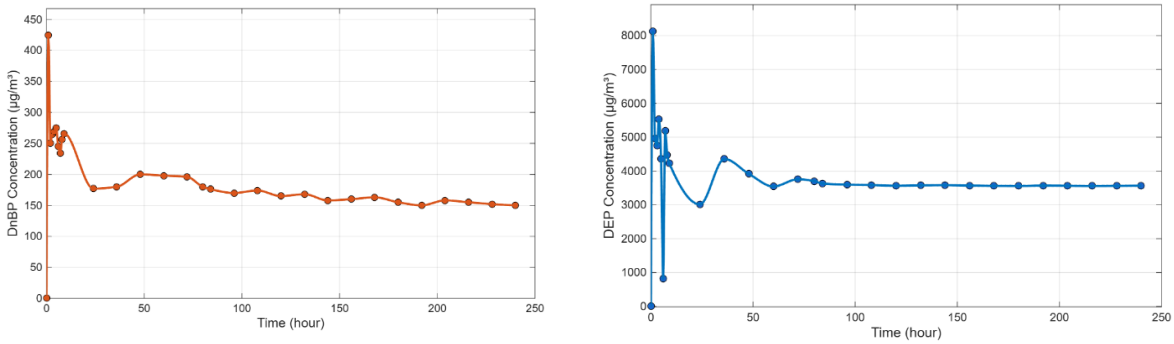

Figure 4.1. Measured DnBP (left) and DEP (rights) concentration from the outlet of the generator system.

4.2.2 Determining K_p values

The high outlet concentration of DEP was diluted 25 times with clean air before mixing in order to achieve a similar concentration to DnBP.

The K_p values were obtain using Equation 2.1 by integrating measured DEP and DnBP (C_g) concentration. The K_p values for these compounds were in agreement with those values reported in the literature (14,76). The results illustrate a clear increasing trend in the K_p values for both

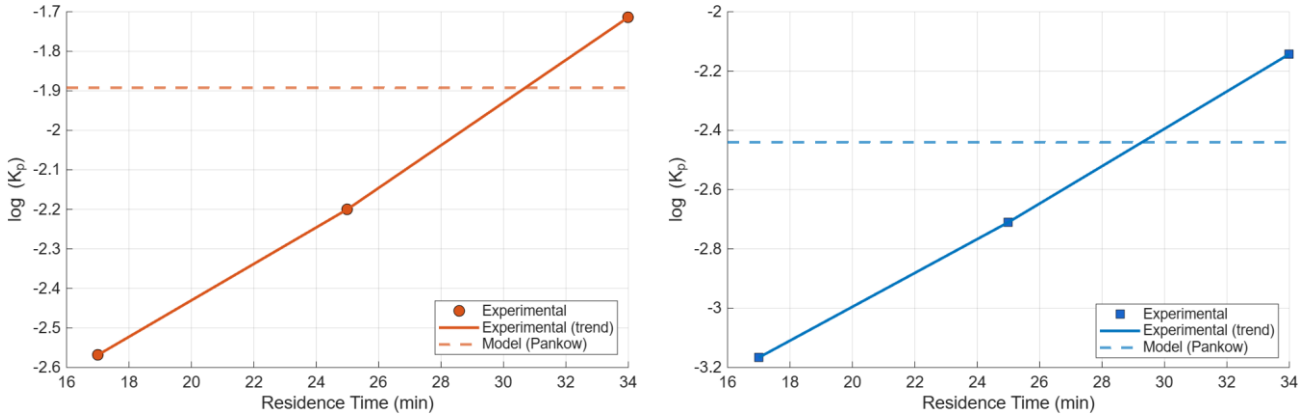

Figure 4.2. K_p values of DnBP (left) and DEP (right) for NaCl particles at different residence time and their predicted values from Pankow adsorption model.

DnBP and DEP as residence time increases from 17 to 34 minutes (Figure 4.2). This suggests that ventilation rate (residence time) significantly affects the equilibrium distribution of SVOCs between the gas and particle phases. For DnBP, K_p values rise from 0.0027 to 0.019 $m^3/\mu g$ at 17 and 34 minutes, respectively, indicating a nearly seven-fold increase. Similarly, for DEP, K_p values experienced an increasing trend from 0.00068 to 0.0071 $m^3/\mu g$ over the same residence time range. Values of parameters used in the adsorption model are tabulated in table 4.1.

Table 4.1. Adsorption model parameter.

Parameter	Value	Notes
Particle median diameter (nm)	337	measured
Particle number concentration (TSP) (#/cm^3)	1×10^6	measured
Total particle surface area (Θ) (cm^2/cm^3)	6.82×10^{-3}	calculated
Total suspended particle (TSP) ($\mu g/m^3$)	395	measured
DnBP vapor pressure (Pa)	2.5×10^{-2}	estimated from mean value (22)
DEP vapor pressure (Pa)	1.8×10^{-1}	estimated from mean value (22)
Constant value for DnBP (Pa.cm)	18.57	measured from (121)
Constant value for DEP (Pa.cm)	37.86	measured from (121)

4.2.3 Effect of AER

Figure 4.2 shows that longer residence times (lower AER) result in higher SVOC partitioning onto particles. This phenomenon can be applied to the dynamics of SVOC partitioning. At longer residence times, there is more time for gaseous SVOCs to interact with and adsorb onto PMs,

resulting in higher K_p values. In contrast, at shorter residence times, the system is likely experiencing enhanced ventilation or turbulence, reducing the time available for equilibrium partitioning, leading to higher gas-phase concentration of SVOCs. As can be seen from Figure 4.2. the model prediction tends to ignore the effect of time residence. These results suggested that besides particles and SVOCs' properties (as introduced in adsorption models), the residence time has a strong influence on K_p values.

4.3 Discussion

While Equation 2.3 defines K_p as an equilibrium parameter, the experimental K_p values can change over time due to non-equilibrium partitioning. Pankow suggested that at equilibrium the rates of sorption and evaporation of SVOC molecules to/from particulate matter are balanced K_p representing the equilibrium ratio. Nevertheless, when the contact time between gaseous SVOC molecules and available sites on particles is limited, the interaction may not reach equilibrium (in this case residence time of 17 and 25 min). In our experimental condition, where inorganic NaCl particles were used, interaction between particles and SVOC molecules occurs at the particles surface through physical adsorption processes. Consequently, the equilibration between gas phase and particle phase depends on the contact time which in this case is a function of residence time (or air exchange rate). The change in K_p values in Figure 4.2 suggests that particle residence time is shorter than the equilibration time, which leads to non-equilibrium condition. Therefore, measured K_p can evolve over time in a dynamic experiment with residence time as the sorption-desorption kinetics are time dependent.

From Figure 4.2, shorter residence time (17 and 25 min) did not reach the model prediction, meaning that the partitioning was not reached to equilibrium. However, for the longest residence

time (34 min), measured K_p values surpassed model predictions. This discrepancy might be due to two main factors. Firstly, in calculating particle surface area, an assumption was made that the particle is cubic, and sorption occurs only on the external surface. In reality, these particles might have different morphological shape and might have different surface characteristics, such as porosity. Irregular morphology can lead to higher surface area for SVOC to partition on the particle surface and pores can bring about more SVOC to penetrate inside the wall of pores. Consequently, the actual surface area and the sorption capacity of NaCl particles might be more than predicted by the idealized cubic geometry, which can lead to higher measured K_p. Secondly, in Pankow's model another assumption was set by which SVOC partition on the particle by monolayer adsorption process. Nevertheless, at longer residence time, SVOCs might have enough time to adsorb in multimolecular layers which can lead to shaping a thin organic layer covering the particle surface and can bring about creating a mixed adsorption–absorption regime. This film can cause enhanced partitioning beyond monolayer capacity and can increase measured K_p.

The partitioning ratio is thermodynamically linked to vapor pressure through a nonlinear Clausius-Clapeyron relationship (122). This relationship reflects not only the vapor pressure of the compound but also the enthalpy of the desorption (Q1) from the available site on the particle surface (reflecting how strong the interaction is). Consequently, this can affect the ratio of enthalpy of desorption to enthalpy of vaporization which in turn it can affect the constant in Equation 2.3. Zhou et al. experimentally confirmed that temperature has a strong negative relationship with K_p (76). As in this study the temperature was kept constant, the effect of temperature on the partitioning ratio was investigated.

Hygroscopic inorganic particles, such as NaCl, tend to absorb moisture from air at high relative humidity. This sorption only happens above a certain level of humidity, called deliquescence

relative humidity (DRH). Above this point, humidity can alter the properties of inorganic particles such as NaCl by forming a liquid film surrounding the particle surface and by dissolving itself in the volume of the sorbed water. This can affect the size of particle and its tendency to adsorb organic molecules such as SVOCs. However, humidity in this study was kept constant at 15 %, which is significantly lower than NaCl molecules' DRH point (at 20 ºC this value is 75.5%), indicating adsorption occurred on crystalline NaCl surfaces. Zhou et al. also reported that humidity has lower effects on K_p values than temperature. Therefore, with low humidity conducted in this study, it is safe to say that humidity has minor effect on partitioning process.

Another factor that can affect the partitioning process is by particle properties including particle surface area, size distribution and composition. For inorganic particles, surface area is a cornerstone factor which is reflected in Pankow's model (Θ). Smaller particles with higher surface area provide more available surface for SVOCs' adsorption (121). Particle composition can affect the partitioning process by shifting from adsorption to absorption (61) which has been shown that organic particles (absorption) lead to higher K_p values in compare with inorganic particles (adsorption). In this study, the properties of particles were nearly identical which led to isolating these factors to see the influence of AER.

4.4 Conclusion

This study examines the particle-gas partitioning behaviour of two phthalates (DnBP and DEP) with an inorganic particle (NaCl) in a mixing chamber. Experimental data illustrated that DnBP has higher K_p value than DEP, due to its lower vapor pressure and its greater affinity for particle phase. The results suggested that AER can affect K_p values for inorganic particles, which challenged the previous assumptions that AER can only influence organic particles due to diffusion

limitation of SVOCs across organic film around the particle. Moreover, these results indicated that the effect of AER on K_p is more highlighted for lower vapor pressure compounds (DnBP). The experimental findings aligned with theoretical predictions only for shorter period.

5 Phthalate Particle-gas Partitioning of Inorganic Particles: Effect of Particle Size and Phthalate Adsorption Competition

In modern life, people spend most of their time in indoor environments. This makes indoor air quality a pivotal factor for safeguarding public health. Therefore, understanding the behavior of air pollutants is vital for ensuring healthy indoor air. Phthalates, a subgroup of semi-volatile organic compounds (SVOCs), are widely used as plasticizers in numerous consumer products, including personal care products and medical devices (98,99). Because of their potential negative health effects including respiratory diseases (123,124) and developmental disruption (125,126), understanding their behavior in indoor environments is critical for public health risk assessments (127). As these compounds are not chemically bonded to consumer products (128), they gradually escape from products leading to their omnipresence in the environment including indoors. One of the influential factors of indoor phthalate contamination is the interaction between the gas-phase phthalate and particulate matter (PM) in the air (129), through which their transport dynamics (13), deposition behavior, and human inhalation exposure can be assessed (130).

Particle-gas partitioning is an essential criterion to evaluate such interaction (7,131), which can be quantified by its particle-gas partition coefficient K_p ($m^3/\mu g$) (132). This coefficient has a direct application in indoor fate-transport models studies (82,133) and in human SVOCs exposure estimates studies (134). Particle-gas partitioning is a physical process governed by intermolecular forces between particles and SVOC molecules (135). One of the important factors influencing this process is the size of particles (136). Not only does particle size influence the K_p values (110), but also it affects airborne residence time and deposition dynamics of SVOCs (137) as larger particles fallout faster while the finer ones remain suspended longer in the air.

In atmospheric studies, research has been conducting experiments to observe the size-dependent sorption behavior of different classes of SVOCs (30,37,42). For instance, low molecular weight (LMW) polycyclic aromatic hydrocarbons (PAHs) adsorb/absorb more onto/into larger particles (67), while high molecular weight (HMW) PAHs onto/into particles with finer size ranges such as nanoparticles (66). Allen et al. (69) suggested that it is driven by the higher volatility of lighter compounds and size-specific chemical affinities of SVOCs. Mandalakis et al. (70) reported the same trend for brominated flame retardants (BFRs) like polybrominated diphenyl ethers (PBDEs).

Hu et al. (71) used a size-segregating samplers, Micro-Orifice Uniform Deposit Impactor (MOUDI), to separate airborne particles based on their sizes. By doing so, they showed that phthalates and organophosphate esters (OPEs) had bimodal particle size distributions. Notably, K_p values for these compounds were greatest in the submicron range of 0.1 – 0.32 μm. Conversely, coarse particles may exhibit greater uptake of SVOCs when the source of emission involves mechanical abrasion or direct resuspension. This indicates a dual mechanism of partitioning—adsorption and absorption—that vary with particle size.

Although prior studies have provided an overview of the behavior of SVOCs towards different particle sizes, several unknowns remain. Because most previous studies collected samples from ambient air, with a mixed composition of particles, the size effect on partitioning has been difficult to isolate from other factors. In fact, particle composition, which has a direct effect on particle-gas partitioning (61), can change with particle size (138), leading to change in the affinity of the selected compounds towards particles of different sizes, and subsequently introducing biases when determining size effects on particle-gas partitioning. Moreover, SVOCs collections in most studies were conducted under different sampling conditions including fluctuation in temperature which can also influence the partitioning of SVOCs. As a result, a seemingly ambiguous relationship

between SVOC partitioning and particle size can be observed in the literature. For example, Su et al. (139) measured K_p values of atmospheric polybrominated diphenyl ether (PBDE) and found that light congeners dominated in fine particles in clear conditions, but all PBDE congeners were found uniformly present in coarse particles during hazy episodes, indicating that the particle size in the latter situation had a diminished influence on partitioning.

The aim of this study is to investigate the effects of particle size on SVOC partitioning by selecting pure inorganic particles (sodium chloride) and constant environmental conditions (temperature and relative humidity) to control possible confounding factors. Furthermore, this study aims to assess competition among phthalates during adsorption to the particle. Understanding these dynamics is key to improving models to predict indoor air quality and refining human exposure assessments.

5.1 Equations to describe particle-gas partitioning coefficients

The particle-gas partitioning coefficient was experimentally driven by Equation 2.1. By substituting the Equation 2.1 in Equation 2.2 the following formula can be derived (22) for comparing the results with previous adsorption model studies :

$$\log(K_p) = log\frac{C_J.\Theta}{TSP} - \log(P^0) \quad (5.1)$$

Aerosol particles generated by nebulization of aqueous NaCl solutions and subsequent drying are usually of cubic shape (140). With an assumption that NaCl particles are cubic, the surface area of a single particle (A_p) with a dimension of d_p (cm) can be calculated as:

$$A_p = 6\, d_p^2 \tag{5.2}$$

Therefore, the total surface area (Θ, cm^2/cm^3) of a given particle size can be calculated by the sum of products of A_s and number of particles (N_{tsp}, $\#/cm^3$) in each particle bin.

$$\Theta = \sum N_{tsp,i}.A_{p,i} \tag{5.3}$$

5.2 Adsorption model parameters

The model K_p values were obtained using Equation 5.1, by integrating the vapor pressure (P^0) of phthalate (Table 3.1) and properties of particles (Table 5.1). To be consistent with earlier studies (141) a value of 17.2 Pa.cm was used for C_J *in* evaluation of model K_p .

Table 5.1. Parameters used in the adsorption model.

Parameter	**Particle mean diameter (nm)**			**Notes**
	337	**650**	**1007**	
Total particle surface area (Θ) (m^2/m^3)	$(9.46 \pm 0.63) \times 10^{-2}$	$(4.05 \pm 0.13) \times 10^{-2}$	$(4.24 \pm 0.41) \times 10^{-1}$	Calculated (Eq. 5.2 and Eq. 5.3)
Total suspended particle (TSP) ($\mu g/m^3$)	415 ± 3.5	373.5 ± 10.4	396.3 ± 15.5	Measured

5.3 Methodology

For achieving proposed objectives, the following steps was undertaken. Gaseous phthalates were generated separately using the porous media method described in chapter 3 for DEP, DnBP, BzBP, and DEHP. After primary evaluation of constant concentration, the generated selected phthalate was introduced to the mixing chamber with selected size range of particle. NaCl was selected as a model inorganic particle for the following reasons: 1) NaCl particles are relatively easy to generate in different size ranges to meet the objective of the study, 2) Its particle density is well known; this allows better control of particles' surface area at constant mass concentrations, 3) Marine aerosols have been found as a dominant compound in various regions (142,143). Although NaCl is generated naturally from sea spray, it represents a simplified inorganic particle without organic coating, and 4) Isolating particle composition to inorganic particles leads to observing changes in K_p values over particle size ranges. NaCl particle in the range of 300-375 nm, 579-721 nm and 897-1117 nm were generated by using different the aqueous NaCl solution concentration (see chapter 3). Figure 5.1 depicts the size distribution of particles from each solution.

Then after by measuring the total and gas-phase concentration of selected phthalate the experimental K_p value was calculated. The constant value using in the model (C_J) also was calculated by measuring the total surface area of particle, knowing the TSP concentration, the vapor pressure of the compound, and K_p value of the selected particle size. Although indoor humidity mostly ranges from 40-60%, in this study a low humidity level was maintained to avoid potential growth of NaCl particle size in the mixing chamber. Previous studies also indicated that humidity has minimal effect on the partitioning (144).

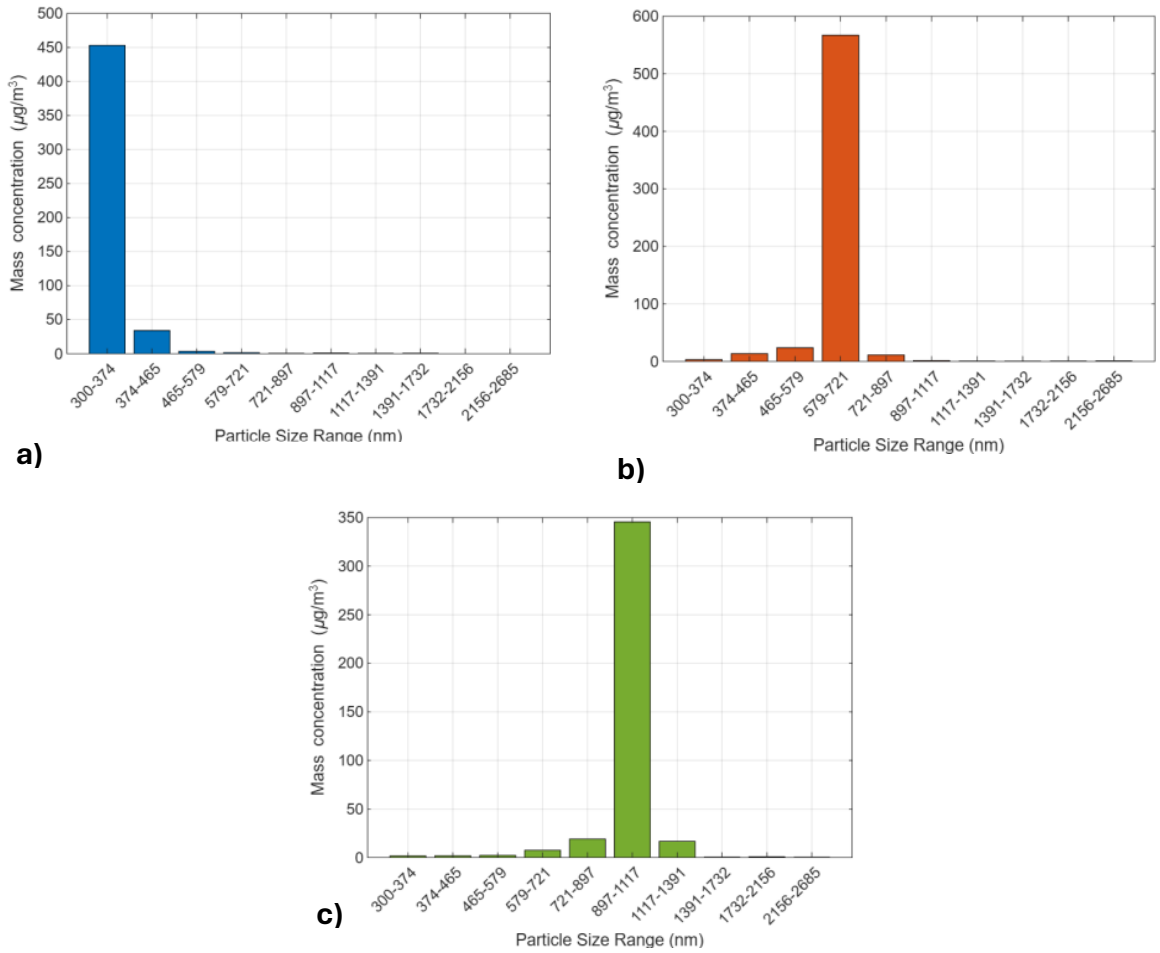

Figure 5.1. Distribution of generated particle mass concentration in each bin. from 350 mg/L (a), 500 mg/L (b), 600 mg/L (c) of NaCl in water.

5.4 Results

5.4.1 Generating gaseous phthalates

The stability of the phthalates generator system was evaluated by running and monitoring phthalate levels over a 10-day period. The generated phthalate concentrations at the outlet of the generator system at 20 °C were 3626.3 ± 291 μg/m^3, 149 ± 8.3 μg/m^3, 28 ± 1.7 μg/m^3, and 1.4 ± 0.5 μg/m^3 for DEP, DnBP, BzBP and DEHP, respectively (Figure 5.2, left side y-axis). To minimize the impact of phthalate concentration on the partitioning, more consistent levels of phthalates, similar to those of DnBP were generated. For DEP, this was achieved by diluting generated DEP 25 times with the clean air to achieve a concentration of 145.04 ± 11.64 μg/m^3 (Figure 5.2a, right side y-

axis). For BzBP and DEHP, a hot plate was used to heat the generator to 33 ºC and 57 ºC for BzBP and DEHP, respectively, to generate BzBP and DEHP concentration of 153 ± 9.6 µg/m^3, and 148 ± 11.3 µg/m^3, respectively (y-scale at right side in Figure 5.2c and 5.2d). Concentrations of the stable range (100 to 200 hours) were used for studying particle-gas partitioning.

a)

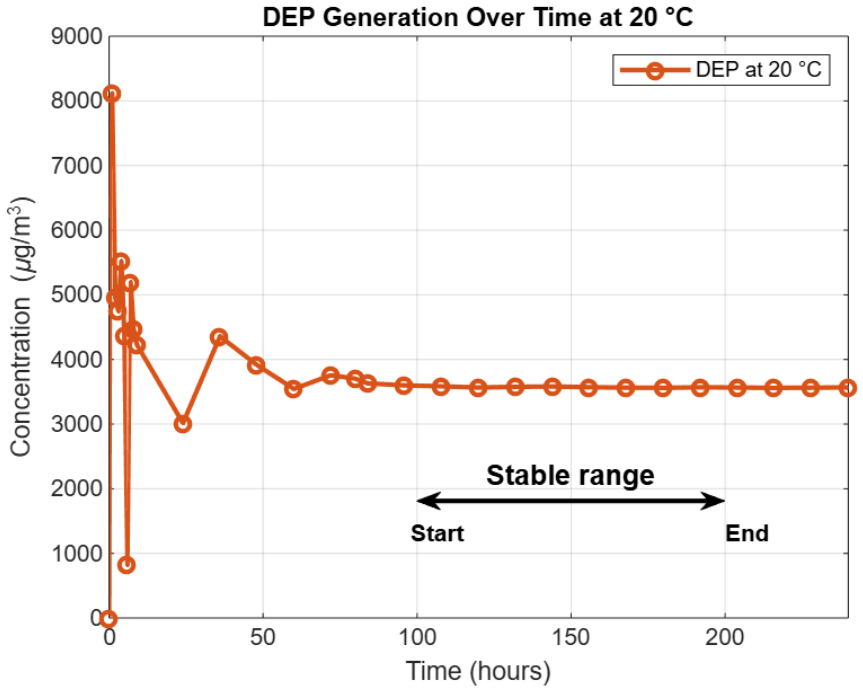

b)

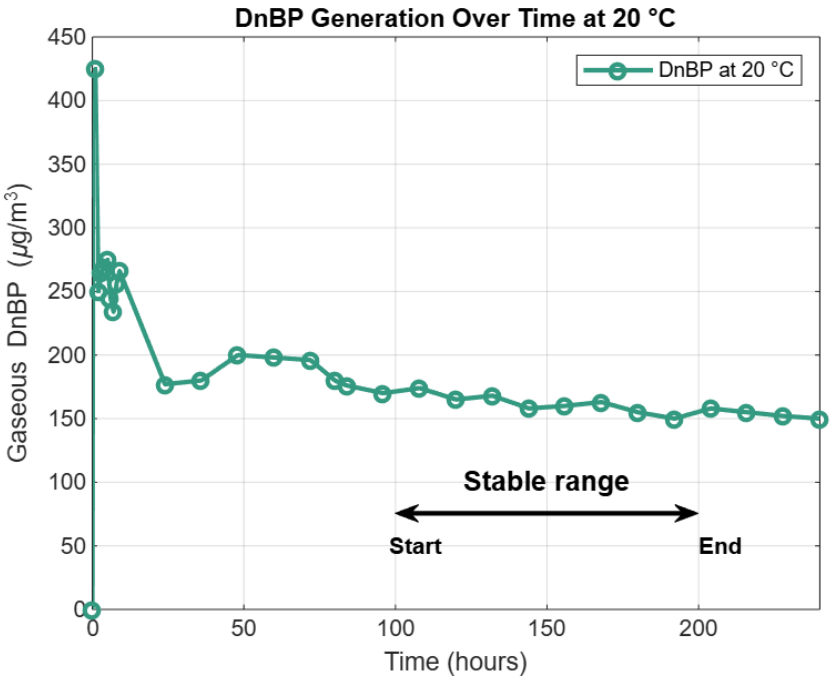

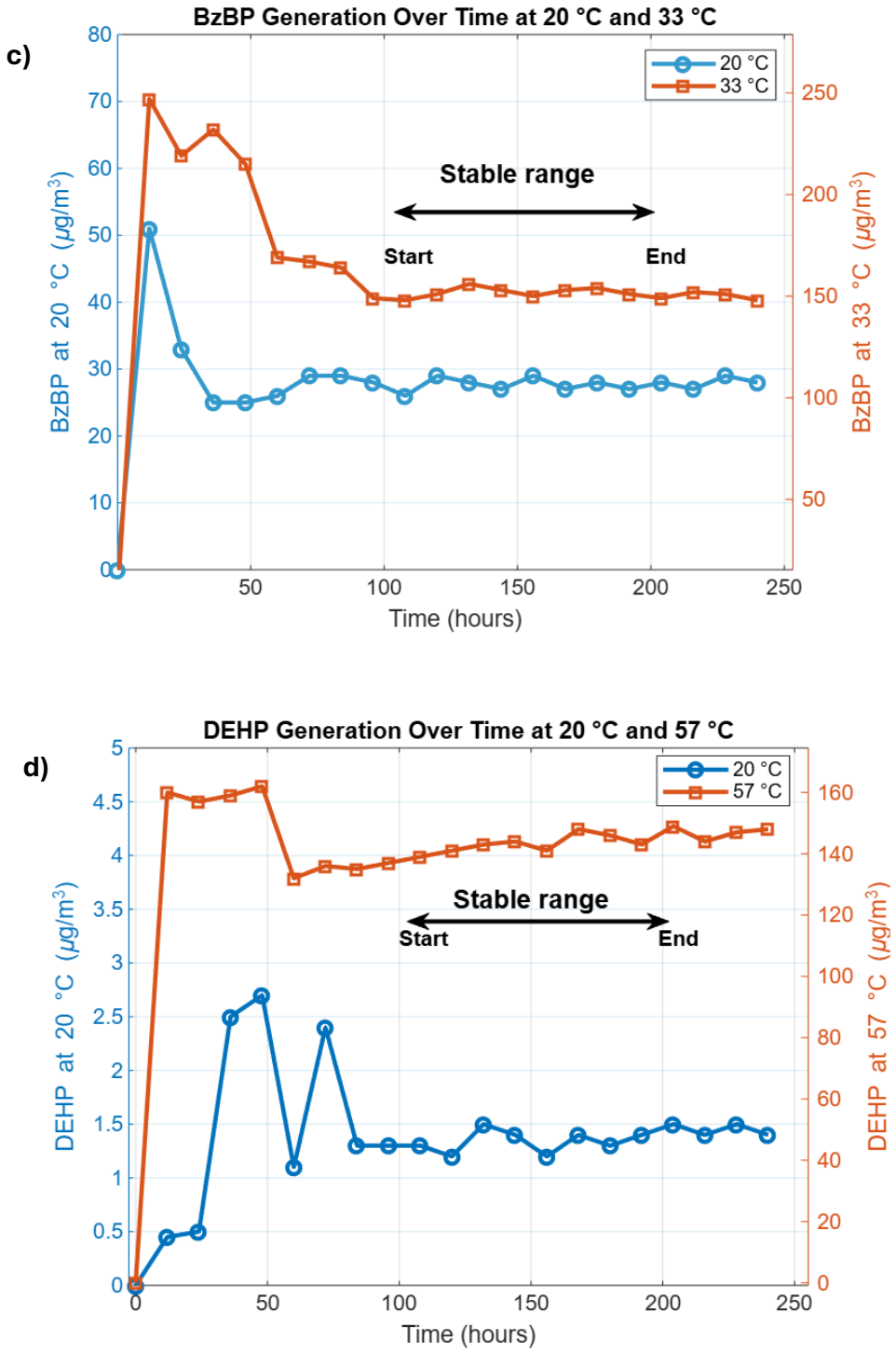

Figure 5.2. Gaseous phthalates concentrations from the outlet of generators system for DEP (a), DnBP (b), BzBP at 20 ºC and 33 ºC (c), and for DEHP at 20 ºC and 57 ºC (d). Arrows indicate the stable range of generated concentrations (100 to 200 hours).

Table 5.2. Experimentally determined K_p values (Equation 2.1) and Const. Values (Equation 2.3) for four selected phthalates at three particle sizes.

	K_p ($m^3/\mu g$)			C_J (Pa.cm)		
Particle size	337 nm	650 nm	1007 nm	337 nm	650 nm	1007 nm
DEP	$(0.594 \pm 0.023) \times 10^{-3}$	$(0.487 \pm 0.019) \times 10^{-3}$	$(0.417 \pm 0.028) \times 10^{-3}$	37.86	33.67	30.58
DnBP	$(1.29 \pm 0.13) \times 10^{-3}$	$(0.954 \pm 0.018) \times 10^{-3}$	$(0.787 \pm 0.038) \times 10^{-3}$	18.57	19.38	19.21
BzBP	$(6.91 \pm 0.19) \times 10^{-3}$	$(5.48 \pm 0.26) \times 10^{-3}$	$(4.78 \pm 0.15) \times 10^{-3}$	15.13	17.35	20.04
DEHP	$(9.05 \pm 0.15) \times 10^{-2}$	$(8.27 \pm 0.11) \times 10^{-2}$	$(7.25 \pm 0.16) \times 10^{-2}$	17.93	18.83	18.91

5.4.2 Determining K_p values

Calculated K_p values from measured C_p, C_g and TSP values (Equation 2.1) for phthalates in three particle size range are presented in Table 5.2. The observed K_p values were in the trend of DEHP > BzBP > DnBP > DEP. The results showed that less volatile compounds such as DEHP had higher K_p values indicating their stronger affinity towards inorganic particles. Particle size influences the partition coefficient value; for all four tested phthalates, log (K_p) decreased with increasing particles size from 337 nm to 1007 nm. This is because larger particles (at fixed mass concentration) provide less surface area for adsorption (145). For instance, DEP (with highest vapor pressure among the four test phthalates) had mean log (K_p) of -3.2 at 337 nm declining to -

3.4 at 1007 nm while DEHP (with lowest vapor pressure) had mean log (K_p) of -1.04 at 337 nm falling to -1.14 at 1007 nm.

Comparisons of experimentally determined K_p values (Equation 2.1) and model predictions (Equation 5.1) for each phthalate in three particle sizes are illustrated in Figure 5.3. The value of constant in the prediction model was obtained from Equation. 5.1. Good agreement between model predicted and experimentally determined K_p values was achieved, except for DEP where the model underestimated the K_p values for DEP by 0.4 Log units. This underestimation of DEP's K_p (0.4 Log units), however, is in the acceptable range suggested by previous model studies where the acceptable deviation range was set to be ±1 Log unit (82,146).

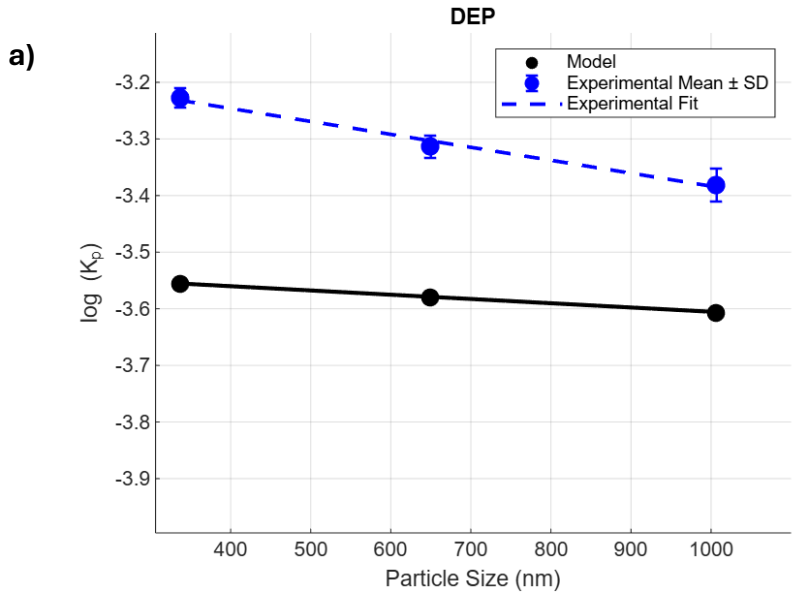

b)

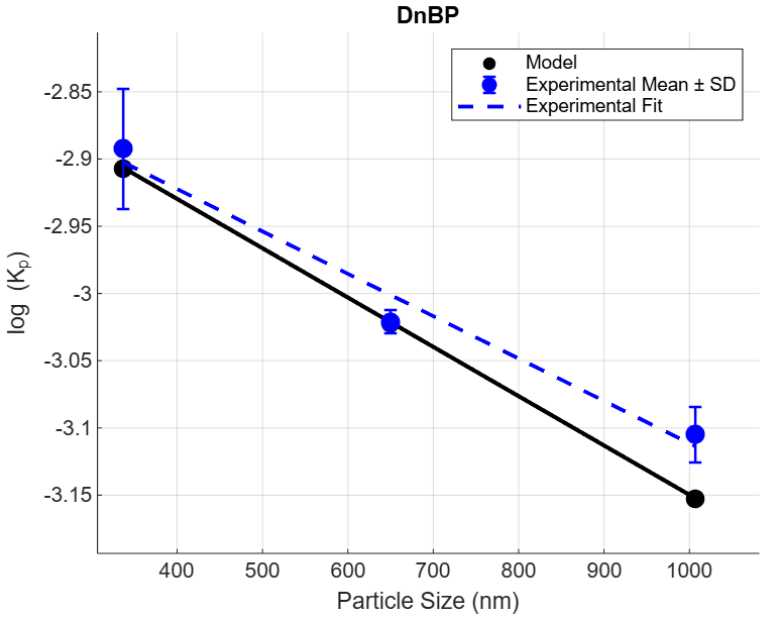
DnBP
Model
Experimental Mean ± SD
Experimental Fit
log (Kp)
-2.85
-2.9
-2.95
-3
-3.05
-3.1
-3.15
400
500
600
700
800
900
1000
Particle Size (nm)

c)

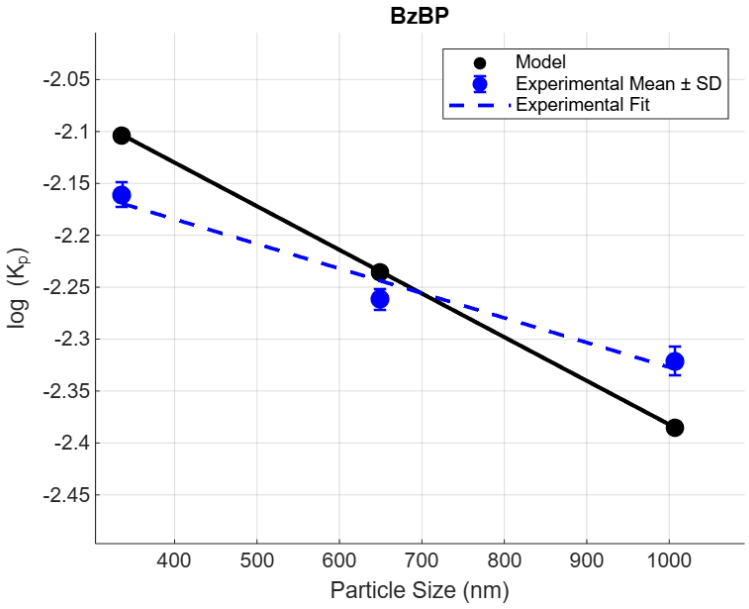
BzBP
Model
Experimental Mean ± SD
Experimental Fit
log (Kp)
-2.05
-2.1
-2.15
-2.2
-2.25
-2.3
-2.35
-2.4
-2.45
400
500
600
700
800
900
1000
Particle Size (nm)

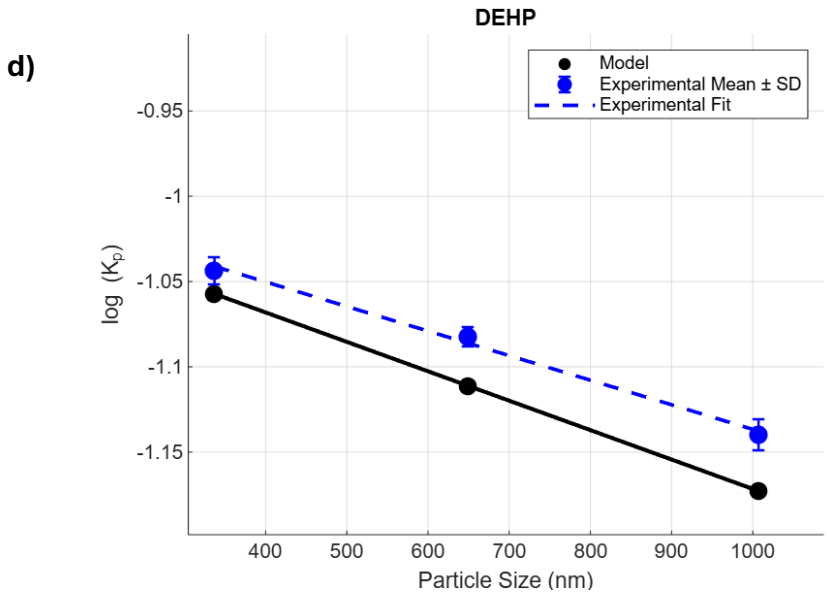

Figure 5.3. Comparisons of experimental K_p values with adsorption model for DEP (a), DnBP (b), BzBP (c), and DEHP (d). For model prediction, a Const. value of 17.2 cited from (39) is used in the model prediction.

5.4.3 Correlation of Log (K_p) and Log (P^0)

Figure 5.4 depicts that for all three particle sizes (337 nm, 650 nm, and 1007 nm), the linear fits of Log (K_p) versus Log (P^0) possessed slopes close to -1 (-0.871, -0.882, and -0.886, respectively) with coefficients of determination (R^2) greater than 0.975. A slope value of -1 in this case indicates the particle-gas partitioning process of phthalates is dominated by adsorption (37). Pankow suggested that such slope is consistent with both adsorption and absorption; however, depending on an increase in Const. value or an increase in fraction of organic matters on particles, one can say that which mechanism is dominant (adsorption or absorption). For particles with low organic matters, they concluded that an intercept value range of -8.9 to -7.3 indicates an absorption dominated portioning process (47). In this case, as the fraction of organic matter is zero, the value of slope shows that adsorption is the main mechanism. It was also observed that the intercept value decreased from -4.08 to -4.26 with increased particle size from 337 nm to 1007 nm.

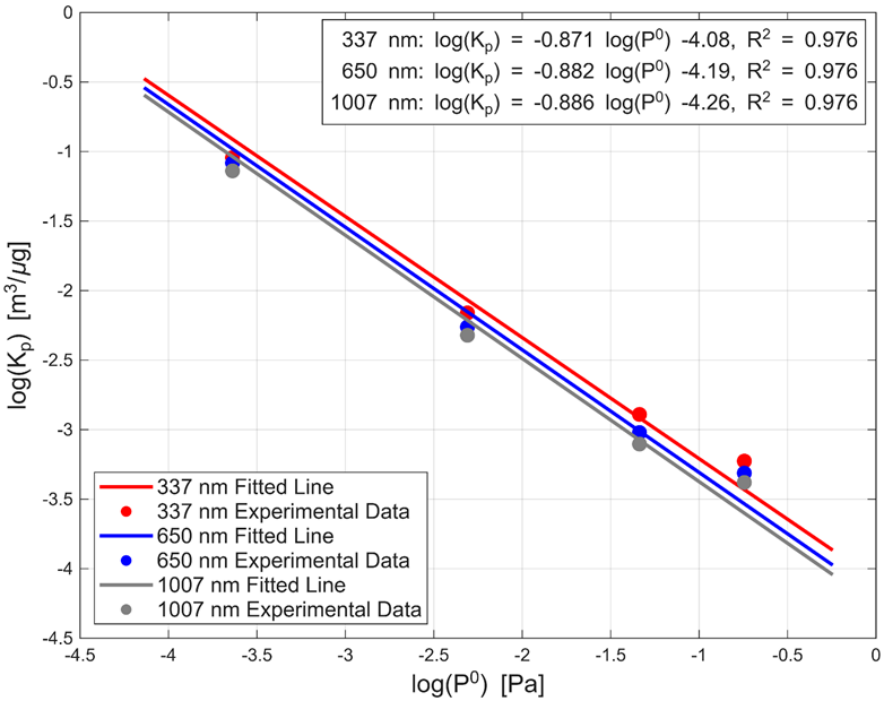

Figure 5.4. Log (K_p) versus Log (P^0) for four tested phthalates in three NaCl particle sizes centered at; 337 nm (red), 650 nm (blue), and 1007 nm (grey).

5.4.4 Phthalate competition for adsorption

DnBP was generated at a steady concentration of 73 ± 5.1 µg/m^3, and the BzBP generation rate was 80 ± 4.2 µg/m^3 which was generated at 33 °C (Figure 5.5). Although the concentration of individual phthalate was reduced due to lower airflow passing through the generators (250 ml/min) the sum of the two (153 µg/m^3) was similar to the levels of the experiments for individual phthalates. The K_p values for the binary mix of selected phthalates were calculated from Equation 2.1. The collection system followed the same procedure as the previous section with the exception that collection time was increased to 25 min. After mixing DnBP and BzBP with particles having diameter of 1007 nm the particle-gas partitioning coefficients of DnBP and BzBP were 0.000677 ± 0.000023 and 0.00442 ± 0.00013 m^3/µg, respectively. Compared to single phthalate, there was

a drop in K_p value in the mixture situation by the factor of 0.86 and 0.93 for DnBP and BzBP, respectively.

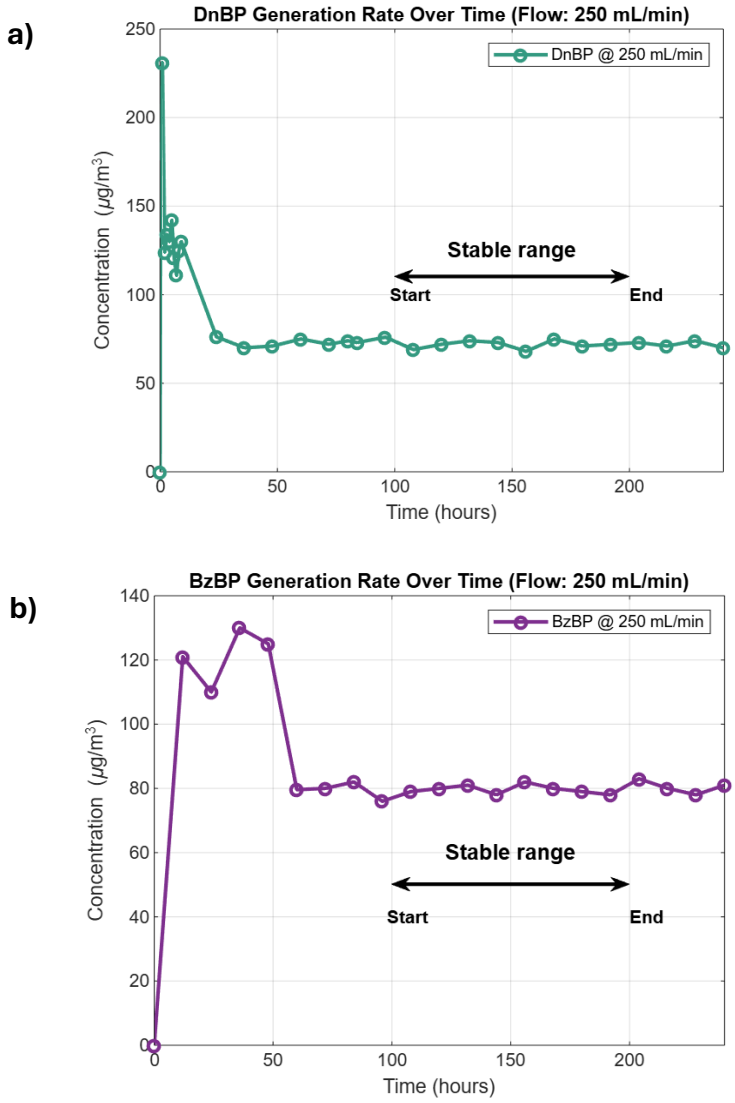

Figure 5.5. Generated gaseous DnBP at 20 ºC (a) and BzBP at 33 ºC (b) with a flow of 250 ml/min for each generator. Arrows indicate the stable range of concentrations (100 to 200 hours) where data were used to determine K_p values.

5.5 Discussion

K_p values of phthalates have been reported in previous atmospheric studies (36,147,148). Although our results in general agree with previous reported values, there are some differences. For example,

K_p values for DnBP were in the range of 8.23×10-4 to 1.15×10-3 $m^3/\mu g$ as opposed to the range of 1.0×10-4 to 6.6×10-3 $m^3/\mu g$ provided by Wang et al. (14). DEHP possessed higher K_p values in this study (0.082 ± 0.0075 $m^3/\mu g$) in comparison to the one Wu et al. (61) calculated for the compound towards inorganic ammonium sulfate particles (0.011 ± 0.004 $m^3/\mu g$). This difference could be attributed to the different types of the particles in the two studies; it was reported that the affinity of the SVOCs adsorption differs depending of the type of soot particle (141). Another reason might be because a mixing chamber was used in this study and a tube chamber coated with DEHP was used by Wu et al. Using a mixing chamber in this enhances the interaction between phthalates and inorganic particles resulting in higher K_p values.

For the same mass concentration of TSP, the particle number concentration depends on the particle size as more surface area is available in smaller size particles on per mass basis. This has a direct effect on the particle-gas partitioning processes. For indoor behaviour of phthalates, Wang et al. (14) showed that phthalates with log (P^0) less than -2.5 (in our case DEHP) tended to enrich in both extremely fine (100 nm to 320 nm) and in coarse particles (10 μm to 18 μm) (a bimodal distribution). Particle-gas partitioning is a complex process and is influenced by multiple factors like the properties of the chemicals as well as those of the particles, such as composition and surface morphology. By setting other factors constant and focusing on different particle sizes, the current study has shown clearly an inverse relationship between particle size and partition coefficient of all four test phthalates. This inverse relationship can be largely attributed to the higher surface area per mass of particles associated with smaller size. Comparing experimentally determined K_p values and model predicted ones (Figure 5.3), it is observed that the model predicted more decrease in K_p values against increased particle size. For example, for BzBP the Log (K_p) values determined experimentally were -2.16, -2.26 and -2.33 (a decrease of 0.17 Log units) for

particle size 337 nm, 650 nm and 1007 nm, respectively, while the Log (K_p) values were predicted to be -2.16, -2.35 and -2.57 (a decrease of 0.41 Log units) for the corresponding sizes. The slower than model predicted decline of K_p values in the experiments might be contributed by the deviation of experimental conditions from the assumptions for the establishment of the adsorption model (section 2), and from the deviation from the assumption of cubic NaCl particles. In fact, multilayer adsorption could become significant for smaller particles invalidating the monolayer hypothesis.

Apart from different particle surface area per unit particle mass, another possible reason for the higher K_p values associated with smaller size particles might be due to more efficient diffusion of smaller particles in the airflow, which have higher chance of collusion (interaction) with phthalates. Larger particles due to their inertia follow the streamline of the flow whereas smaller particles due to their light weight can diffuse in the streamline and this can bring about higher potential of interactions. This consideration may be useful in bioavailability and bioaccessibility studies as smaller particles can penetrate occupants' cardiovascular system and can have deleterious effect. Particles with diameter of about 300 nm are recognized as the most penetrating particle size (MPPS) in particle filtration studies and can act as carriers for chemicals to the body.

In this study, a near -1 slope value was observed for Log (K_p) to Log (P^0) for all three sizes of particles (Figure 5.4). The intercept in this case is -4.08, -4.19 and -4.26 for particle size 337 nm, 650 nm and 1007 nm, respectively. These intercept values were comparable but slightly smaller than PAHs in indoor air which is in the range of -4.70 to -4.90 (149). The current study suggests that the intercept is size dependent and the value increases with increasing particle size. This phenomenon is important for indoor air quality as PM amplifies human exposure to SVOCs by partitioning to particles. The size dependent intercept is a key to improve models of indoor air

quality and refining human exposure which can contribute to a better understanding of indoor exposure pathways.

The reduction of K_p values for both DnBP and BzBP originates from the competitive sorption of phthalates for finite surface area (particle sorption capacity). This shows that the selected phthalates do not compete in the same way. As mentioned in the previous section, when mixing single phthalates with particles the K_p value for BzBP was higher than DnBP, meaning that BzBP has higher affinity towards particles due to its lower vapor pressure. In the binary mixture, the compound with higher affinity adsorbs proportionally more to the surface of particles. In fact, the stronger sorbate (BzBP) suppresses the weaker one (DnBP) for occupying the available sites. This was shown by Liang and Pankow for PAHs where K_p values for the mixture of compounds dropped by factor of 0.7 to 1 (150).

In the atmospheric and indoor air studies SVOCs never occur in a single-compound matrix, rather as a complex mixture of SVOCs. While most particle-gas partitioning models still use the single-compound K_p values (23,46,48,49), here, we have demonstrated the importance of considering mixture activity of SVOCs, which can help inform and improve future studies and model development. This will help researchers to improve their estimation of human SVOCs intake, and their fate and transport in both outdoor and indoor environments. The numerical value of Const. in this study was calculated for the four phthalates at three particle sizes. The results show that the Const. is a function of both particle size and SVOCs type. Compound specific Const. values were also observed by others. For example, Lammel et al. reported Const. values in range of 1.3 to 1740 Pa.cm for 10 PAHs (151); those with vapor pressures similar to this study selected phthalates ranged from 4.1 to 102 Pa.cm. Shahpoury et al. reported mean Const. value from 4.49 to 9.5 Pa.cm for the four PAHs, namely phenanthrene, fluoranthene, pyrene and benzo(a)anthracene, that have

similar vapor pressure as the four phthalates in this study in ambient air (141). In this study the Const. values for the phthalates in NaCl (15 to 20 Pa.cm, except in the case of DEP) were higher than those for PAHs in ambient air, but very similar to the 17.2 Pa.cm proposed by Shahpoury et al. for non-specific sorbent (141). The calculated Const. reflects not only the physical interactions between phthalates and particles, but it also shows these interactions are size-dependent. This suggests that Const. is a compound and condition dependent parameter. Our findings support the notion that there is a need to use chemical-specific Const. for more accurate prediction in future studies.

While controlled experiment condition allowed for the clear demonstration of size and composition effects, this study is subject to certain limitations. Firstly, the generated NaCl particles do not reflect the complexity of indoor particles, which are a mix of complex particle compositions (e.g. road dust particles, organics, bioaerosols). Secondly, the two-chemical binary system used for the competitive nature in adsorption is far from the real-world situation in indoor environment where a far more complex mixture of SVOCs from other groups (e.g. PAHs) along with other pollutants is presented. Thirdly, the temperature and humidity were held constant in the experiments although SVOCs partitioning in indoor air is taking place in a more fluctuated temperature and humidity environment.

Findings of this work can have several applications for indoor air management strategies and exposure assessments. The finding showed a decrease in K_p values as particle diameter increased optimized cleaning strategies can be used to remove these pollutants in the airstream as the filtration is a function of particle size. Therefore, knowing the indoor behavior of SVOCs will help us to design and optimize the building air cleaning systems to reduce the indoor SVOCs concentration. As the particle deposition and infiltration into our body is dependent on particle

size, exposure risk assessments can be enhanced by considering this impact. Furthermore, current models for predicting SVOCs partitioning are based on single-compound partitioning. However, partitioning of SVOCs in real-world will not occur in isolation of each other. Our competitive adsorption results showed the competitive sorption must be considered to improve the current prediction models to better reflect the real indoor air situation.

5.6 Summary

In this study, the particle-gas partitioning coefficients of four phthalates (DEP, DnBP, BzBP, DEHP) in size-resolved NaCl particles were experimentally determined in a mixing chamber under controlled conditions. Results showed that the adsorption process dominates the partitioning and K_p depends on both phthalate volatility (vapor pressure) and particle size. Overall, higher molecular-weight compounds (lower vapor pressure, e.g., DEHP) had higher affinity for adsorption to NaCl particles. Besides, the partitioning of all phthalates decreased systematically as the particle diameter shifted from 337 nm to 1007 nm.

This work also provides experimental evidence that competitive interactions between two phthalates can alter partitioning coefficients. This highlights the importance of mixture effects in real-world SVOC partitioning, where current modeling frameworks are predominantly based on single-compound behavior. Considering size-resolved particles and mixture effect of SVOCs into indoor air quality models will strengthen the accuracy of human exposure assessments. Future research can extend these methods to complex particle matrices (including both inorganic and organic particles) to further refine models for describing indoor SVOC fate and transport in indoor air.

6 Conclusions and Recommendations

6.1 Conclusions

The omnipresence of PM in indoor environments facilitates the SVOC emissions from their sources; besides, through particle-gas partitioning processes these two pollutants have interaction by which the exposure of SVOCs can be increased. Both pollutants pose human-health concerns and have particularly deleterious effects on the cardiovascular, pulmonary, and reproductive systems. Although many experimental works have been conducted to quantify the partitioning (mostly in atmospheric conditions), our understanding of how gas-phase SVOCs interact with PM in indoor environments remains limited. Particle properties have been suggested to have an immense effect on the partitioning; however, no studies have investigated this effect under controlled laboratory conditions. For human exposure assessment and indoor air quality management, this is vital. In fact, accurate determination of partitioning (through particle-gas partitioning coefficient) allows for more precise indoor SVOCs fate and transport prediction, which enables the design of more effective exposure mitigation strategies.

This dissertation has been carried out to study how these two pollutants interact in indoor environments. Through three experimental frameworks and model development, this work introduces new quantitative insight and information into how ventilation dynamics, particle size, and binary mixture of phthalates govern the distribution of the gas-phase and particle-phase of SVOCs. These findings can advance not only fundamental understanding but also practical prediction of SVOC behavior in indoor air, which can be considered as a critical step toward more accurate exposure assessment and effective control strategies.

The first objective was to systematically investigate the effect of air exchange rate on partitioning coefficient (K_p) (Chapter 4). It was demonstrated that residence time has a profound effect on the

K_p of diethyl phthalate (DEP) and di-n-butyl phthalate (DnBP). When the ventilation rate increased, results showed that neither compound reached equilibrium and traditional adsorption model overestimated the particulate uptake while increasing residence time to 34 minutes led to underestimation of K_p values. This result highlights the inadequacy of equilibrium assumptions in ventilated indoor environments and suggests an adjustment for existing model frameworks.

The second objective was to determine the role of particle size by conducting partitioning experiments on inorganic generated NaCl particles with three size ranges of 337 nm, 650 nm, and 1000 nm (Chapter 5), and four phthalates—DEP, DnBP, benzyl butyl phthalate (BzBP), and di-2-ethylhexyl phthalate (DEHP) by setting other parameters as constants. K_p values were found to be size dependent and experienced a drop by 20 to 50 percent as particle diameter increased from 337 nm to 1 μm. The inverse relationship reflects the reduction in surface-area-to-volume ratio on larger particles, which can highly affect the effective adsorption sites per unit mass. Moreover, fitting the experimental K_p values, TSP, and vapor pressure of compound revealed that the constant used in adsorption model is compound and size dependent which is aligned with ambient polycyclic aromatic hydrocarbon studies. By knowing the TSP concentration and the number concentration of particles, the constant that was used in traditional models was improved for each target phthalates and particle size. The observed size dependence suggests that coarse particles have different interaction with SVOCs compared with fine particle. This finding is pivotal for both bioavailability and bioaccessibility studies as smaller particles can penetrate our cardiovascular system. Fine particles with a diameter of 300 nm can also penetrate the filtration system due to their light weight and their diffusion in streamline of air. Therefore, our findings are useful for future remediation strategies in indoor air quality domain.

The last objective was to determine the effect of binary mixture of DnBP and BzBP on a particle. This research revealed the competitive adsorption effects whereas the individual partitioning coefficients dropped by up to 30 percent (Chapter 5). When both compounds were introduced into the mixing chamber the higher-vapor pressure compound tended to suppress the partitioning of lower-vapour pressure compound. Competitive adsorption likely arises from differences in molecular polarity, vapor pressure, and surface affinity, where lower-volatility compounds (in this case BzBP) exhibit stronger binding to inorganic surfaces and may block sorption sites for the lighter one (in this case DnBP). Similar competitive behaviors have been reported in atmospheric aerosol and mineral-surface interaction studies, where limited adsorption sites and heterogeneous surface energies promote preferential uptake of more surface-active species. These results suggest that multilayer adsorption and surface-site competition may play a role in SVOC mixtures, particularly for inorganic particle systems. This has been done for the first time in partitioning studies while earlier studies carried out on a single-compound condition. In real indoor environments, a complex mixture of SVOCs (species like PCBs and PAHs) is presented, while models were developed for a single-compound interaction and neglected this effect.

Beyond improving K_p prediction, this work developed the practical methodologies that can be used for other SVOCs that exist as liquids at room temperature. The use of mixing chamber with control airflow can mimic the indoor spaces where SVOCs and particles have plenty time of interaction. The SVOCs generation system provides high reproducibility and stability over the course of experiments. Using the sorbent tube sampling minimized positive and negative artifacts, improving confidence in measured both gas and particle-phase concentration of SVOCs. Therefore, the methodological approach can be applied to other SVOCs and both inorganic and organic particles with isolated parameters by which the effect of targeted parameter can be likely

investigated. Each factor contributes uniquely to model accuracy and their combined implementation bridges the gap between controlled laboratory measurements and the dynamic complexity of real indoor air. With continued refinement and expansion, this work will enable researchers and engineers to better understand and control the behavior of SVOCs pollutants in the environment.

6.2 Recommendations for future work

Despite abovementioned advances, several limitations still exist that need to be addressed in future work. We specifically propose the following future research to refine predictive capabilities of the models and expand their applicability:

1) Mixed inorganic-organic aerosols are present in the real indoor environment. Studying these complex particles can help distinguish the relative contributions of absorption (into the bulk phase) versus adsorption (onto the surface) in the partitioning behavior of SVOCs. Future studies can be extended to not only a mixture of inorganic and organic particles but also a more realistic scenario by adding dust. In fact, dust is a pivotal exposure route for children by ingestion pathways which makes its partitioning with SVOCs vital to consider. Besides, it can become airborne by human activity (e.g. vacuum cleaner) and can contribute more to particle-phase SVOCs in indoor spaces. In such system, SVOCs may interact via gas-phase sorption as well as through direct contact or abrasion from their sources. Therefore, future studies can consider variety of dust types (e.g. collected from bag of vacuum cleaner, standard dust like Arizona one) from different temperature zones. Choosing the collection location is also important (e.g. school, hospital, office etc.) to have better exposure assessment in such places.

2) As particles possess different morphology based on their size and their composition, it is important to study this effect on SVOCs particle-gas partitioning behavior. In the current study, the morphology of generated particles was assumed to be cubic while particles often possess irregular shapes, porosity and complex internal surfaces structure. These features can impact both the available adsorption surface area, which can directly have impact on sorption and evaporation rate of SVOCs from the surface of particle, and the diffusion pathways within the porous structure of particles. For achieving this goal, future studies can be expanded on using different particle generation methods, such as using combustion-generated soot or diesel exhaust particle, which will generate irregular, fractal-like, highly porous particles. Experimental studies using advanced imaging techniques (e.g., SEM, AFM) and BET surface area analysis will help quantify these effects on gas-particle partitioning.

3) Investigation of the effects of particle's properties on other SVOC classes (e.g., flame retardants, PAHs) with wider spectrum of vapor pressures is another aspect to study. As some groups present in solid form under room conditions, the future work should be expanded on generating solid based compound by sublimation techniques using a permeation chamber (housing the compound) which is immersed in a thermostatic water bath to control outlet concentration. By developing a reliable method to generate gaseous SVOCs from their solid form, the current approach (liquid form) can be combined with the new method to study the particle-gas partitioning of other groups. The tentative experiments can be expanded on adsorption (or absorption) mixture dependencies.

4) The measured K_p values from this study can be incorporated into whole-building indoor air quality modeling frameworks, such as multi-zone mass-balance models or computational fluid dynamics (CFD) simulations. K_p values can be used to evaluate how HVAC system, occupant behavior, and building conditions interact to influence the concentration and distribution of

SVOCs in both gas and particle phases. This will provide a more realistic understanding of occupational exposure pathways and will enable engineers to choose optimized strategies for different building types and scenarios (e.g. ventilation rates, filter selection, and material choices in building) to ensure healthier indoor environments.

References

1. Lu J, Wu J, Chen Y. Indoor environment and brain health across the life course: A systematic review. Building and Environment. 2025 Jan 1;267:112156.

2. Saraga DE, Querol X, Duarte RMBO, Aquilina NJ, Canha N, Alvarez EG, et al. Source apportionment for indoor air pollution: Current challenges and future directions. Science of The Total Environment. 2023 Nov 20;900:165744.

3. Dodson RE, Camann DE, Morello-Frosch R, Brody JG, Rudel RA. Semivolatile Organic Compounds in Homes: Strategies for Efficient and Systematic Exposure Measurement Based on Empirical and Theoretical Factors. Environ Sci Technol. 2015 Jan 6;49(1):113–22.

4. Xu Y, Liu Z, Park J, Clausen PA, Benning JL, Little JC. Measuring and predicting the emission rate of phthalate plasticizer from vinyl flooring in a specially-designed chamber. Environ Sci Technol. 2012 Nov 20;46(22):12534–41.

5. Zhang X, Wang H, Xu B, Wang H, Wang Y, Yang T, et al. Predicting the emissions of VOCs/SVOCs in source and sink materials: Development of analytical model and determination of the key parameters. Environment International. 2022 Feb 1;160:107064.

6. Liu X, Guo Z, Roache NF. Experimental method development for estimating solid-phase diffusion coefficients and material/air partition coefficients of SVOCs. Atmospheric Environment. 2014 Jun 1;89:76–84.

7. Bahrami A, Haghighat F, Zhu J. Indoor environment gas-particle partitioning models of SVOCs and impact of particle properties on the partitioning: A review. Building and Environment. 2024 Aug 15;262:111791.

8. Liu C, Zhang Y, Weschler CJ. Exposure to SVOCs from Inhaled Particles: Impact of Desorption. Environ Sci Technol. 2017 Jun 6;51(11):6220–8.

9. Sonne C, Xia C, Dadvand P, Targino AC, Lam SS. Indoor volatile and semi-volatile organic toxic compounds: Need for global action. Journal of Building Engineering. 2022 Dec 15;62:105344.

10. Liu C, Zhang Y, Weschler CJ. Exposure to SVOCs from Inhaled Particles: Impact of Desorption. Environ Sci Technol. 2017 Jun 6;51(11):6220–8.

11. Weschler CJ, Nazaroff WW. SVOC partitioning between the gas phase and settled dust indoors. Atmospheric Environment. 2010 Sep 1;44(30):3609–20.

12. Eichler CMA, Bi C, Wang C, Little JC. A modular mechanistic framework for estimating exposure to SVOCs: Next steps for modeling emission and partitioning of plasticizers and PFAS. J Expo Sci Environ Epidemiol. 2022 May;32(3):356–65.

13. Liang Y, Bi C, Wang X, Xu Y. A general mechanistic model for predicting the fate and transport of phthalates in indoor environments. Indoor Air. 2019;29(1):55–69.

14. Wang SQ, Hu YJ, Yuan YF, Hu ZC, Wu CC, Bao LJ, et al. Size-resolved gas-particle partitioning characteristics of typical semi-volatile organic compounds in urban atmosphere. Environmental Pollution. 2023 Mar 1;320:121101.

15. He J, Balasubramanian R. A study of gas/particle partitioning of SVOCs in the tropical atmosphere of Southeast Asia. Atmospheric Environment. 2009 Sep 1;43(29):4375–83.

16. Wei W, Mandin C, Blanchard O, Mercier F, Pelletier M, Le Bot B, et al. Temperature dependence of the particle/gas partition coefficient: An application to predict indoor gas-phase concentrations of semi-volatile organic compounds. Science of The Total Environment. 2016 Sep 1;563–564:506–12.

17. Kristensen K, Lunderberg DM, Liu Y, Misztal PK, Tian Y, Arata C, et al. Gas–Particle Partitioning of Semivolatile Organic Compounds in a Residence: Influence of Particles from Candles, Cooking, and Outdoors. Environ Sci Technol. 2023 Feb 28;57(8):3260–9.

18. Wang Z, Na G, Ma X, Fang X, Ge L, Gao H, et al. Occurrence and gas/particle partitioning of PAHs in the atmosphere from the North Pacific to the Arctic Ocean. Atmospheric Environment. 2013 Oct 1;77:640–6.

19. Zhu FJ, Ma WL, Liu LY, Zhang ZF, Song WW, Hu PT, et al. Temporal trends of atmospheric PAHs: Implications for the gas-particle partition. Atmospheric Environment. 2021 Sep 15;261:118595.

20. Salthammer T, Goss KU. Predicting the Gas/Particle Distribution of SVOCs in the Indoor Environment Using Poly Parameter Linear Free Energy Relationships. Environ Sci Technol. 2019 Mar 5;53(5):2491–9.

21. Qin M, Yang PF, Hu PT, Hao S, Macdonald RW, Li YF. Particle/gas partitioning for semi-volatile organic compounds (SVOCs) in level III multimedia fugacity models: Both gaseous and particulate emissions. Science of The Total Environment. 2021 Oct 10;790:148012.

22. Salthammer T, Schripp T. Application of the Junge- and Pankow-equation for estimating indoor gas/particle distribution and exposure to SVOCs. Atmospheric Environment. 2015 Apr 1;106:467–76.

23. Harner T, Bidleman TF. Octanol−Air Partition Coefficient for Describing Particle/Gas Partitioning of Aromatic Compounds in Urban Air. Environ Sci Technol. 1998 May 1;32(10):1494–502.

24. Goss KU, Schwarzenbach RP. Linear Free Energy Relationships Used To Evaluate Equilibrium Partitioning of Organic Compounds. Environ Sci Technol. 2001 Jan 1;35(1):1–9.

25. Weschler CJ, Nazaroff WW. Semivolatile organic compounds in indoor environments. Atmospheric Environment. 2008 Dec 1;42(40):9018–40.

26. Li YF, Ma WL, Yang M. Prediction of gas/particle partitioning of polybrominated diphenyl ethers (PBDEs) in global air: A theoretical study. Atmospheric Chemistry and Physics. 2015 Feb 18;15(4):1669–81.

27. Wei X, Yuan Q, Serge B, Xu T, Ma G, Yu H. In silico investigation of gas/particle partitioning equilibrium of polybrominated diphenyl ethers (PBDEs). Chemosphere. 2017 Dec 1;188:110–8.

28. Yamasaki H, Kuwata K, Miyamoto H. Effects of ambient temperature on aspects of airborne polycyclic aromatic hydrocarbons. Environ Sci Technol. 1982 Apr 1;16(4):189–94.

29. Pankow JF. An absorption model of the gas/aerosol partitioning involved in the formation of secondary organic aerosol. Atmospheric Environment. 1994 Jan 1;28(2):189–93.

30. He W, Liu WX, Qin N, Kong XZ, He QS, Xu FL. Impact of organic matter and meteorological factors on the long-term trend, seasonality, and gas/particle partitioning behavior of atmospheric PBDEs. Science of The Total Environment. 2019 Apr 1;659:1058–70.

31. Melymuk L, Bohlin P, Sáňka O, Pozo K, Klánová J. Current Challenges in Air Sampling of Semivolatile Organic Contaminants: Sampling Artifacts and Their Influence on Data Comparability. Environ Sci Technol. 2014 Dec 16;48(24):14077–91.

32. Woolfenden E. Sorbent-based sampling methods for volatile and semi-volatile organic compounds in air: Part 1: Sorbent-based air monitoring options. Journal of Chromatography A. 2010 Apr 16;1217(16):2674–84.

33. Melymuk L, Bohlin-Nizzetto P, Prokeš R, Kukučka P, Přibylová P, Vojta Š, et al. Uncertainties in monitoring of SVOCs in air caused by within-sampler degradation during active and passive air sampling. Atmospheric Environment. 2017 Oct 1;167:553–65.

34. Benning JL, Liu Z, Tiwari A, Little JC, Marr LC. Characterizing Gas-Particle Interactions of Phthalate Plasticizer Emitted from Vinyl Flooring. Environ Sci Technol. 2013 Mar 19;47(6):2696–703.

35. Wu Y, Eichler CMA, Cao J, Benning J, Olson A, Chen S, et al. Particle/Gas Partitioning of Phthalates to Organic and Inorganic Airborne Particles in the Indoor Environment. Environ Sci Technol. 2018 Mar 20;52(6):3583–90.

36. Huang L, Qiao Y, Deng S, Zhou M, Zhao W, Yue Y. Airborne phthalates in indoor environment: Partition state and influential built environmental conditions. Chemosphere. 2020 Sep 1;254:126782.

37. Zhang BZ, Guan YF, Li SM, Zeng EY. Occurrence of Polybrominated Diphenyl Ethers in Air and Precipitation of the Pearl River Delta, South China: Annual Washout Ratios and Depositional Rates. Environ Sci Technol. 2009 Dec 15;43(24):9142–7.

38. Genisoglu M, Sofuoglu A, Kurt-Karakus PB, Birgul A, Sofuoglu SC. Brominated flame retardants in a computer technical service: Indoor air gas phase, submicron (PM1) and coarse (PM10) particles, associated inhalation exposure, and settled dust. Chemosphere. 2019 Sep 1;231:216–24.

39. Callén MS, de la Cruz MT, López JM, Murillo R, Navarro MV, Mastral AM. Some inferences on the mechanism of atmospheric gas/particle partitioning of polycyclic aromatic hydrocarbons (PAH) at Zaragoza (Spain). Chemosphere. 2008 Nov 1;73(8):1357–65.

40. Akyüz M, Çabuk H. Gas–particle partitioning and seasonal variation of polycyclic aromatic hydrocarbons in the atmosphere of Zonguldak, Turkey. Science of The Total Environment. 2010 Oct 15;408(22):5550–8.

41. Wang W, Simonich SLM, Wang W, Giri B, Zhao J, Xue M, et al. Atmospheric polycyclic aromatic hydrocarbon concentrations and gas/particle partitioning at background, rural village and urban sites in the North China Plain. Atmospheric Research. 2011 Feb 1;99(2):197–206.

42. Yu H, Yu JZ. Polycyclic aromatic hydrocarbons in urban atmosphere of Guangzhou, China: Size distribution characteristics and size-resolved gas-particle partitioning. Atmospheric Environment. 2012 Jul 1;54:194–200.

43. Barhoumi B, Guigue C, Touil S, Johnson-Restrepo B, Driss MR, Tedetti M. Hydrocarbons in the atmospheric gas phase of a coastal city in Tunisia: Levels, gas–particle partitioning, and health risk assessment. Science of The Total Environment. 2023 Jun 25;879:162986.

44. Junge C. Basic considerations about trace constituents in the atmosphere as related to the fate of global pollutants. Advances in environmental science and technology [Internet]. 1977 [cited 2023 Oct 30]; Available from: https://www.semanticscholar.org/paper/Basic-considerations-about-trace-constituents-in-as-Junge/fc60cef5abd389f7e59c72cdcf06c5d1743f1fa4

45. Pankow JF. Review and comparative analysis of the theories on partitioning between the gas and aerosol particulate phases in the atmosphere. Atmospheric Environment (1967). 1987 Jan 1;21(11):2275–83.

46. Dachs J, Eisenreich SJ. Adsorption onto Aerosol Soot Carbon Dominates Gas-Particle Partitioning of Polycyclic Aromatic Hydrocarbons. Environ Sci Technol. 2000 Sep 1;34(17):3690–7.

47. Abraham MH. Scales of solute hydrogen-bonding: their construction and application to physicochemical and biochemical processes. Chem Soc Rev. 1993 Jan 1;22(2):73–83.

48. Goss KU. Predicting the equilibrium partitioning of organic compounds using just one linear solvation energy relationship (LSER). Fluid Phase Equilibria. 2005 Jun 15;233(1):19–22.

49. Endo S, Goss KU. Applications of Polyparameter Linear Free Energy Relationships in Environmental Chemistry. Environ Sci Technol. 2014 Nov 4;48(21):12477–91.

50. Götz CW, Scheringer M, MacLeod M, Roth CM, Hungerbühler K. Alternative Approaches for Modeling Gas−Particle Partitioning of Semivolatile Organic Chemicals: Model Development and Comparison. Environ Sci Technol. 2007 Feb 1;41(4):1272–8.

51. Shahpoury P, Lammel G, Albinet A, Sofuoğlu A, Dumanoğlu Y, Sofuoğlu SC, et al. Evaluation of a Conceptual Model for Gas-Particle Partitioning of Polycyclic Aromatic Hydrocarbons Using Polyparameter Linear Free Energy Relationships. Environ Sci Technol. 2016 Nov 15;50(22):12312–9.

52. Jang M, Czoschke NM, Lee S, Kamens RM. Heterogeneous Atmospheric Aerosol Production by Acid-Catalyzed Particle-Phase Reactions. Science. 2002 Oct 25;298(5594):814–7.

53. Vander Wal RL, Bryg VM, Hays MD. XPS Analysis of Combustion Aerosols for Chemical Composition, Surface Chemistry, and Carbon Chemical State. Anal Chem. 2011 Mar 15;83(6):1924–30.

54. Huang RJ, Zhang Y, Bozzetti C, Ho KF, Cao JJ, Han Y, et al. High secondary aerosol contribution to particulate pollution during haze events in China. Nature. 2014 Oct;514(7521):218–22.

55. Srivastava D, Vu TV, Tong S, Shi Z, Harrison RM. Formation of secondary organic aerosols from anthropogenic precursors in laboratory studies. npj Clim Atmos Sci. 2022 Mar 24;5(1):1–30.

56. Zhang R, Wang G, Guo S, Zamora ML, Ying Q, Lin Y, et al. Formation of Urban Fine Particulate Matter. Chem Rev. 2015 May 27;115(10):3803–55.

57. Zhou X, Luo C, Wang X, Liu K. Simplified methods for characterizing dynamic sorption of SVOCs on viscous particles. Atmospheric Environment. 2020 Nov 15;241:117796.

58. Andersen HV, Bramming Jørgensen R, Gunnarsen L. Impact of smoking and candle burning on air concentrations of PCB in a PCB contaminated indoor environment. Atmospheric Environment. 2023 Sep 15;309:119922.

59. Bi C, Wang X, Li H, Li X, Xu Y. Direct Transfer of Phthalate and Alternative Plasticizers from Indoor Source Products to Dust: Laboratory Measurements and Predictive Modeling. Environ Sci Technol. 2021 Jan 5;55(1):341–51.

60. Kondo K, Kagi N, Namiki N. Study on the mechanism of SVOC adsorption onto airborne particles in indoor air. JAPAN ARCHITECTURAL REVIEW. 2018;1(4):528–37.

61. Wu Y, Eichler CMA, Cao J, Benning J, Olson A, Chen S, et al. Particle/Gas Partitioning of Phthalates to Organic and Inorganic Airborne Particles in the Indoor Environment. Environ Sci Technol. 2018 Mar 20;52(6):3583–90.

62. Liu C, Shi S, Weschler C, Zhao B, Zhang Y. Analysis of the Dynamic Interaction Between SVOCs and Airborne Particles. Aerosol Science and Technology. 2013 Feb 1;47(2):125–36.

63. Strommen MR, Kamens RM. Development and Application of a Dual-Impedance Radial Diffusion Model to Simulate the Partitioning of Semivolatile Organic Compounds in Combustion Aerosols. Environ Sci Technol. 1997 Oct 1;31(10):2983–90.

64. Shiraiwa M, Zuend A, Bertram AK, Seinfeld JH. Gas–particle partitioning of atmospheric aerosols: interplay of physical state, non-ideal mixing and morphology. Phys Chem Chem Phys. 2013 Jun 18;15(27):11441–53.

65. Thomas D, Charvet A. 1 - An Introduction to Aerosols. In: Thomas D, Charvet A, Bardin-Monnier N, Appert-Collin JC, editors. Aerosol Filtration [Internet]. Elsevier; 2017 [cited 2021 Jul 12]. p. 1–30. Available from: https://www.sciencedirect.com/science/article/pii/B9781785482151500019

66. Shen G, Wang W, Yang Y, Ding J, Xue M, Min Y, et al. Emissions of PAHs from Indoor Crop Residue Burning in a Typical Rural Stove: Emission Factors, Size Distributions, and Gas−Particle Partitioning. Environ Sci Technol. 2011 Feb 15;45(4):1206–12.

67. Tian M, Liang B, Zhang L, Hu H, Yang F, Peng C, et al. Measurement of size-segregated airborne particulate bound polycyclic aromatic compounds and assessment of their human health impacts - A case study in a megacity of southwest China. Chemosphere. 2021 Dec 1;284:131339.

68. Gu Y, Xu H, Feng R, Zhang B, Gao M, Sun J, et al. Insight into personal exposure characteristics and health effects of PM2.5 and PM0.25-bound PAHs and their derivatives with different heating ways in the Fenwei Plain, China. Environmental Pollution. 2023 Dec 1;338:122699.

69. Allen JO, Dookeran NM, Smith KA, Sarofim AF, Taghizadeh K, Lafleur AL. Measurement of Polycyclic Aromatic Hydrocarbons Associated with Size-Segregated Atmospheric Aerosols in Massachusetts. Environ Sci Technol. 1996 Feb 1;30(3):1023–31.

70. Mandalakis M, Besis A, Stephanou EG. Particle-size distribution and gas/particle partitioning of atmospheric polybrominated diphenyl ethers in urban areas of Greece. Environmental Pollution. 2009 Apr 1;157(4):1227–33.

71. Hu PT, Su PH, Ma WL, Zhang ZF, Liu LY, Song WW, et al. New equation to predict size-resolved gas-particle partitioning quotients for polybrominated diphenyl ethers. Journal of Hazardous Materials. 2020 Dec 5;400:123245.

72. Clausen PA, Liu Z, Kofoed-Sørensen V, Little J, Wolkoff P. Influence of Temperature on the Emission of Di-(2-ethylhexyl)phthalate (DEHP) from PVC Flooring in the Emission Cell FLEC. Environ Sci Technol. 2012 Jan 17;46(2):909–15.

73. Liang Y, Caillot O, Zhang J, Zhu J, Xu Y. Large-scale chamber investigation and simulation of phthalate emissions from vinyl flooring. Building and Environment. 2015 Jul 1;89:141–9.

74. Liang Y, Xu Y. Emission of Phthalates and Phthalate Alternatives from Vinyl Flooring and Crib Mattress Covers: The Influence of Temperature. Environ Sci Technol. 2014 Dec 16;48(24):14228–37.

75. Chen Z, Afshari A, Mo J. A method using porous media to deliver gas-phase phthalates rapidly and at a constant concentration: Effects of temperature and media. Environmental Pollution. 2020 Jul 1;262:113823.

76. Zhou X, Lian J, Cheng Y, Wang X. The gas/particle partitioning behavior of phthalate esters in indoor environment: Effects of temperature and humidity. Environmental Research. 2021 Mar 1;194:110681.

77. Pratt GC, Herbrandson C, Krause MJ, Schmitt C, Lippert CJ, McMahon CR, et al. Measurements of gas and particle polycyclic aromatic hydrocarbons (PAHs) in air at urban, rural and near-roadway sites. Atmospheric Environment. 2018 Apr 1;179:268–78.

78. Ma WL, Zhu FJ, Hu PT, Qiao LN, Li YF. Gas/particle partitioning of PAHs based on equilibrium-state model and steady-state model. Science of The Total Environment. 2020 Mar 1;706:136029.

79. Qiao LN, Hu PT, Macdonald R, Kannan K, Nikolaev A, Li YF. Modeling gas/particle partitioning of polybrominated diphenyl ethers (PBDEs) in the atmosphere: A review. Science of The Total Environment. 2020 Aug 10;729:138962.

80. Yin F, He Z, Song Z, Zhang W, Li X, Qin B, et al. Gas-particle partitioning of polycyclic aromatic hydrocarbons from oil combustion involving condensate, diesel and heavy oil. Ecotoxicology and Environmental Safety. 2022 Sep 1;242:113866.

81. Qiao LN, Ma WL, Liu LY, Zhang ZF, Song WW, Jia HL, et al. Particle/gas partitioning behavior of polychlorinated biphenyls (PCBs) in global atmosphere: Equilibrium or steady state? Atmospheric Environment. 2022 Feb 1;270:118926.

82. Li HL, Yang PF, Liu LY, Gong BB, Zhang ZF, Ma WL, et al. Steady-State Based Model of Airborne Particle/Gas and Settled Dust/Gas Partitioning for Semivolatile Organic Compounds in the Indoor Environment. Environ Sci Technol. 2022 Jun 21;56(12):8373–83.

83. Wang X, Bi C, Xu Y. Modeling and analysis of sampling artifacts in measurements of gas-particle partitioning of semivolatile organic contaminants using filter-sorbent samplers. Atmospheric Environment. 2015 Sep 1;117:99–109.

84. Melymuk L, Bohlin-Nizzetto P, Prokeš R, Kukučka P, Klánová J. Sampling artifacts in active air sampling of semivolatile organic contaminants: Comparing theoretical and measured artifacts and evaluating implications for monitoring networks. Environmental Pollution. 2016 Oct 1;217:97–106.

85. Tsapakis M, Stephanou EG. Collection of gas and particle semi-volatile organic compounds: use of an oxidant denuder to minimize polycyclic aromatic hydrocarbons degradation during high-volume air sampling. Atmospheric Environment. 2003 Nov 1;37(35):4935–44.

86. Bedjanian Y, Nguyen ML, Le Bras G. Kinetics of the reactions of soot surface-bound polycyclic aromatic hydrocarbons with the OH radicals. Atmospheric Environment. 2010 May 1;44(14):1754–60.

87. Pehnec G, Jakovljević I, Šišović A, Bešlić I, Vađić V. Influence of ozone and meteorological parameters on levels of polycyclic aromatic hydrocarbons in the air. Atmospheric Environment. 2016 Apr 1;131:263–8.

88. Omelekhina Y, Eriksson A, Canonaco F, Prevot ASH, Nilsson P, Isaxon C, et al. Cooking and electronic cigarettes leading to large differences between indoor and outdoor particle composition and concentration measured by aerosol mass spectrometry. Environ Sci: Processes Impacts. 2020 Jun 24;22(6):1382–96.

89. Cousins IT, Mackay D, Parkerton TF. Physical-Chemical Properties and Evaluative Fate Modelling of Phthalate Esters. In: Series Anthropogenic Compounds [Internet]. Springer, Berlin, Heidelberg; 2003 [cited 2025 May 14]. p. 57–84. Available from: https://link.springer.com/chapter/10.1007/b11463

90. Wang R, Zhu J, Rastan S, Haghighat F. Measuring chemical emissions from wet products—Development of a new measurement technique. Journal of Hazardous Materials. 2011 Sep 15;192(3):1026–32.

91. Huang H, Haghighat F, Blondeau P. Volatile organic compound (VOC) adsorption on material: influence of gas phase concentration, relative humidity and VOC typeAbstract. Indoor Air. 2006;16(3):236–47.

92. Young AS, Allen JG, Kim UJ, Seller S, Webster TF, Kannan K, et al. Phthalate and Organophosphate Plasticizers in Nail Polish: Evaluation of Labels and Ingredients. Environ Sci Technol. 2018 Nov 6;52(21):12841–50.

93. Xue J, Cai H, Li W, Pei Y, Guan H, Guo Z, et al. Emissions of VOCs and SVOCs from polyvinyl chloride building materials: Contribution to indoor odor and inhalation health risks. Building and Environment. 2023 Feb 1;229:109958.

94. Li Y, Zhang S, Guo Z, Wang L, Qiao L, Chen Y, et al. An in-situ versatile screening method for identifying SVOC sources in indoor environments. Environment International. 2024 Jul 1;189:108794.

95. Grindler NM, Vanderlinden L, Karthikraj R, Kannan K, Teal S, Polotsky AJ, et al. Exposure to Phthalate, an Endocrine Disrupting Chemical, Alters the First Trimester Placental Methylome and Transcriptome in Women. Sci Rep. 2018 Apr 17;8(1):6086.

96. Caldwell JC. DEHP: Genotoxicity and potential carcinogenic mechanisms—A review. Mutation Research/Reviews in Mutation Research. 2012 Oct 1;751(2):82–157.

97. Liu GR, Shi GL, Zhang P, Zhou LD, Wu JH, Feng YC. Source identification and toxicity assessment of polycyclic aromatic hydrocarbons in particulate matter of Chengdu, China. Zhongguo Huanjing Kexue/China Environmental Science. 2014;34(10):2479–84.

98. Monti M, Fasano M, Palandri L, Righi E. A review of European and international phthalates regulation: focus on daily use products. European Journal of Public Health. 2022 Oct 1;32(Supplement_3):ckac131.226.

99. Lucattini L, Poma G, Covaci A, de Boer J, Lamoree MH, Leonards PEG. A review of semi-volatile organic compounds (SVOCs) in the indoor environment: occurrence in consumer products, indoor air and dust. Chemosphere. 2018 Jun 1;201:466–82.

100. Rauert C, Harrad S, Suzuki G, Takigami H, Uchida N, Takata K. Test chamber and forensic microscopy investigation of the transfer of brominated flame retardants into indoor dust via abrasion of source materials. Sci Total Environ. 2014 Sep 15;493:639–48.

101. US EPA O. Technical Overview of Volatile Organic Compounds [Internet]. 2014 [cited 2024 Jan 16]. Available from: https://www.epa.gov/indoor-air-quality-iaq/technical-overview-volatile-organic-compounds

102. Eichler CMA, Hubal EAC, Xu Y, Cao J, Bi C, Weschler CJ, et al. Assessing Human Exposure to SVOCs in Materials, Products, and Articles: A Modular Mechanistic Framework. Environ Sci Technol. 2021 Jan 5;55(1):25–43.

103. Raffy G, Mercier F, Glorennec P, Mandin C, Le Bot B. Oral bioaccessibility of semi-volatile organic compounds (SVOCs) in settled dust: A review of measurement methods, data and influencing factors. Journal of Hazardous Materials. 2018 Jun 15;352:215–27.

104. Zeng Y, Chen S, Fan Y, Li Q, Guan Y, Mai B. Effects of carbonaceous materials and particle size on oral and inhalation bioaccessibility of PAHs and OPEs in airborne particles. Environ Sci Pollut Res. 2021 Nov 1;28(44):62133–41.

105. Wei W, Bonvallot N, Gustafsson Å, Raffy G, Glorennec P, Krais A, et al. Bioaccessibility and bioavailability of environmental semi-volatile organic compounds via inhalation: A review of methods and models. Environ Int. 2018 Apr;113:202–13.

106. Xu Y, Little JC. Predicting Emissions of SVOCs from Polymeric Materials and Their Interaction with Airborne Particles. Environ Sci Technol. 2006 Jan 1;40(2):456–61.

107. Liu C, Morrison GC, Zhang Y. Role of aerosols in enhancing SVOC flux between air and indoor surfaces and its influence on exposure. Atmospheric Environment. 2012 Aug 1;55:347–56.

108. Li YF, Qiao LN, Ren NQ, Macdonald RW, Kannan K. Gas/particle partitioning of semi-volatile organic compounds in the atmosphere: Transition from unsteady to steady state. Science of The Total Environment. 2020 Mar 25;710:136394.

109. Salthammer T, Goss KU. Predicting the Gas/Particle Distribution of SVOCs in the Indoor Environment Using Poly Parameter Linear Free Energy Relationships. Environ Sci Technol. 2019 Mar 5;53(5):2491–9.

110. Cao J, Han Y, Zhu Y, Duan X, Wang L, Huang H. Steady-state model for predicting size-resolved gas-particle partitioning of semi-volatile organic compounds (SVOCs) in indoor environments. Build Simul. 2023 Mar;16(3):443–60.

111. Ma WL, Zhu FJ, Hu PT, Qiao LN, Li YF. Gas/particle partitioning of PAHs based on equilibrium-state model and steady-state model. Science of The Total Environment. 2020 Mar 1;706:136029.

112. Qiao LN, Hu PT, Macdonald R, Kannan K, Nikolaev A, Li YF. Modeling gas/particle partitioning of polybrominated diphenyl ethers (PBDEs) in the atmosphere: A review. Science of The Total Environment. 2020 Aug 10;729:138962.

113. Yin F, He Z, Song Z, Zhang W, Li X, Qin B, et al. Gas-particle partitioning of polycyclic aromatic hydrocarbons from oil combustion involving condensate, diesel and heavy oil. Ecotoxicology and Environmental Safety. 2022 Sep 1;242:113866.

114. Melymuk L, Bohlin-Nizzetto P, Prokeš R, Kukučka P, Přibylová P, Vojta Š, et al. Uncertainties in monitoring of SVOCs in air caused by within-sampler degradation during active and passive air sampling. Atmospheric Environment. 2017 Oct 1;167:553–65.

115. Wei W, Ramalho O, Mandin C. A long-term dynamic model for predicting the concentration of semivolatile organic compounds in indoor environments: Application to phthalates. Building and Environment. 2019 Jan 15;148:11–9.

116. Li Y, He L, Xie D, Zhao A, Wang L, Kreisberg NM, et al. Strong temperature influence and indiscernible ventilation effect on dynamics of some semivolatile organic compounds in the indoor air of an office. Environment International. 2022 Jul 1;165:107305.

117. Clausen PA, Liu Z, Xu Y, Kofoed-Sørensen V, Little JC. Influence of air flow rate on emission of DEHP from vinyl flooring in the emission cell FLEC: Measurements and CFD simulation. Atmospheric Environment. 2010 Jul 1;44(23):2760–6.

118. Benning JL, Liu Z, Tiwari A, Little JC, Marr LC. Characterizing Gas-Particle Interactions of Phthalate Plasticizer Emitted from Vinyl Flooring. Environ Sci Technol. 2013 Mar 19;47(6):2696–703.

119. Nguyen LV, Diamond ML, Kalenge S, Kirkham TL, Holness DL, Arrandale VH. Occupational Exposure of Canadian Nail Salon Workers to Plasticizers Including Phthalates and Organophosphate Esters. Environ Sci Technol. 2022 Mar 1;56(5):3193–203.

120. Wei W, Mansouri A, Zoutendijk SL, Langer S, Liagkouridis I, Hopf NB, et al. Plasticizer sources and concentrations in indoor environments in Europe: A systematic review of existing data. Science of The Total Environment. 2025 Apr 1;972:179080.

121. Bahrami A, Haghighat F, Niu J, Zhu J. Phthalates particle-gas partitioning of inorganic particles: Effect of particle size and phthalates adsorption competition. Building and Environment. 2025 Nov 1;285:113619.

122. Hoff RM, Brice KA, Halsall CJ. Nonlinearity in the Slopes of Clausius−Clapeyron Plots for SVOCs. Environ Sci Technol. 1998 Jun 1;32(12):1793–8.

123. Jaakkola JJK, Knight TL. The Role of Exposure to Phthalates from Polyvinyl Chloride Products in the Development of Asthma and Allergies: A Systematic Review and Meta-analysis. Environmental Health Perspectives. 2008 Jul;116(7):845–53.

124. Yu Y, Wang JQ. Phthalate exposure and lung disease: the epidemiological evidences, plausible mechanism and advocacy of interventions. Reviews on Environmental Health. 2024 Mar 1;39(1):37–45.

125. Mesquita I, Lorigo M, Cairrao E. Update about the disrupting-effects of phthalates on the human reproductive system. Molecular Reproduction and Development. 2021;88(10):650–72.

126. Lyche JL, Gutleb ,Arno C., Bergman ,Åke, Eriksen ,Gunnar S., Murk ,AlberTinka J., Ropstad ,Erik, et al. Reproductive and Developmental Toxicity of Phthalates. Journal of Toxicology and Environmental Health, Part B. 2009 Aug 28;12(4):225–49.

127. Dueñas-Moreno J, Mora A, Kumar M, Meng XZ, Mahlknecht J. Worldwide risk assessment of phthalates and bisphenol A in humans: The need for updating guidelines. Environment International. 2023 Nov 1;181:108294.

128. Huang C, Zhang YJ, Liu LY, Wang F, Guo Y. Exposure to phthalates and correlations with phthalates in dust and air in South China homes. Science of The Total Environment. 2021 Aug 15;782:146806.

129. Bu S, Wang Y, Wang H, Wang F, Tan Y. Predicting spatio-temporal distribution of indoor multi-phase phthalates under the influence of particulate matter. Building and Environment. 2022 Aug 1;221:109329.

130. Andersen C, Krais AM, Eriksson AC, Jakobsson J, Löndahl J, Nielsen J, et al. Inhalation and Dermal Uptake of Particle and Gas-Phase Phthalates—A Human Exposure Study. Environ Sci Technol. 2018 Nov 6;52(21):12792–800.

131. Chen Z, Tian E, Jiang Y, Mo J. Global perspectives on indoor phthalates and alternative plasticizers: Occurrence and key transport parameters. Journal of Hazardous Materials. 2025 Jan 15;482:136506.

132. Cao J, Eichler CMA, Wu Y, Little JC. Dynamic method to measure partition coefficient and mass accommodation coefficient for gas–particle interaction of phthalates. Aerosol Science and Technology. 2019 Oct 3;53(10):1158–71.

133. Zhang X, Diamond ML, Robson M, Harrad S. Sources, Emissions, and Fate of Polybrominated Diphenyl Ethers and Polychlorinated Biphenyls Indoors in Toronto, Canada. Environ Sci Technol. 2011 Apr 15;45(8):3268–74.

134. Shi S, Zhao B. Modeled Exposure Assessment via Inhalation and Dermal Pathways to Airborne Semivolatile Organic Compounds (SVOCs) in Residences. Environ Sci Technol. 2014 May 20;48(10):5691–9.

135. Chen Z, Chen Q, Xu Y, Mo J. Partitioning characteristics of indoor VOCs on impermeable surfaces covered by film-phase DnBP and DEHP. Journal of Hazardous Materials Advances. 2022 Nov 1;8:100191.

136. Barbas B, de la Torre A, Sanz P, Navarro I, Artíñano B, Martínez MA. Gas/particle partitioning and particle size distribution of PCDD/Fs and PCBs in urban ambient air. Science of The Total Environment. 2018 May 15;624:170–9.

137. Chen Q, Hu K. Prediction model for SVOCs transport in the air and interactions with airborne particles. Atmospheric Environment. 2014 Oct 1;96:61–9.

138. Glicker HS, Lawler MJ, Ortega J, de Sá SS, Martin ST, Artaxo P, et al. Chemical composition of ultrafine aerosol particles in central Amazonia during the wet season. Atmospheric Chemistry and Physics. 2019 Oct 23;19(20):13053–66.

139. Su P hao, Tomy GT, Hou C yan, Yin F, Feng D lun, Ding Y sheng, et al. Gas/particle partitioning, particle-size distribution of atmospheric polybrominated diphenyl ethers in southeast Shanghai rural area and size-resolved predicting model. Chemosphere. 2018 Apr 1;197:251–61.

140. Krämer L, Pöschl U, Niessner R. Microstructural rearrangement of sodium chloride condensation aerosol particles on interaction with water vapor. Journal of Aerosol Science. 2000 Jun 1;31(6):673–85.

141. Shahpoury P, Lammel G, Albinet A, Sofuoğlu A, Dumanoğlu Y, Sofuoğlu SC, et al. Evaluation of a Conceptual Model for Gas-Particle Partitioning of Polycyclic Aromatic Hydrocarbons Using Polyparameter Linear Free Energy Relationships. Environ Sci Technol. 2016 Nov 15;50(22):12312–9.

142. Almeida SM, Canha N, Silva A, Freitas M do C, Pegas P, Alves C, et al. Children exposure to atmospheric particles in indoor of Lisbon primary schools. Atmospheric Environment. 2011 Dec 1;45(40):7594–9.

143. Tran DT, Alleman LY, Coddeville P, Galloo JC. Elemental characterization and source identification of size resolved atmospheric particles in French classrooms. Atmospheric Environment. 2012 Jul 1;54:250–9.

144. Zhou X, Lian J, Cheng Y, Wang X. The gas/particle partitioning behavior of phthalate esters in indoor environment: Effects of temperature and humidity. Environmental Research. 2021 Mar 1;194:110681.

145. Okuda T. Measurement of the specific surface area and particle size distribution of atmospheric aerosol reference materials. Atmospheric Environment. 2013 Aug 1;75:1–5.

146. Li YF, Qiao LN, Ren NQ, Sverko E, Mackay D, Macdonald RW. Decabrominated Diphenyl Ethers (BDE-209) in Chinese and Global Air: Levels, Gas/Particle Partitioning, and Long-Range Transport: Is Long-Range Transport of BDE-209 Really Governed by the Movement of Particles? Environ Sci Technol. 2017 Jan 17;51(2):1035–42.

147. Wei W, Mandin C, Blanchard O, Mercier F, Pelletier M, Le Bot B, et al. Distributions of the particle/gas and dust/gas partition coefficients for seventy-two semi-volatile organic compounds in indoor environment. Chemosphere. 2016 Jun 1;153:212–9.

148. Lu H, Chen D, Zhu Z, Yang L, Huang L, Xu C, et al. Atmospheric phthalate esters in a multi-function area of Hangzhou: Temporal variation, gas/particle phase distribution, and population exposure risk. Science of The Total Environment. 2023 Oct 10;894:163987.

149. Naumova YY, Offenberg JH, Eisenreich SJ, Meng Q, Polidori A, Turpin BJ, et al. Gas/particle distribution of polycyclic aromatic hydrocarbons in coupled outdoor/indoor atmospheres. Atmospheric Environment. 2003 Feb 1;37(5):703–19.

150. Liang C, Pankow JamesF. Gas/Particle Partitioning of Organic Compounds to Environmental Tobacco Smoke: Partition Coefficient Measurements by Desorption and Comparison to Urban Particulate Material. Environ Sci Technol. 1996 Aug 1;30(9):2800–5.

151. Lammel G, Klánová J, Ilić P, Kohoutek J, Gasić B, Kovacić I, et al. Polycyclic aromatic hydrocarbons in air on small spatial and temporal scales – II. Mass size distributions and gas-particle partitioning. Atmospheric Environment. 2010 Dec 1;44(38):5022–7.